

quencies, just as was done by Anderson for the position-independent case. A possible example is a pair excitation localized and bound near the surface of a superconductor. (The word "bound" implies that the excitation energy lies in the energy gap of the superconductor.) Such a localized pair excitation could occur in the absence of localized single-particle excitations, the position-dependent pairing potential  $\Delta_k(\mathbf{R})$  being capable of binding the former but not the latter.<sup>12</sup>

A second type of dynamic problem solvable with the present formalism is that of the inertia or effective mass associated with a moving normal-superconducting interface. Just as in the analogous ferromagnetic problem of a moving domain wall,<sup>13</sup> the kinetic energy of the interface results from the additional effective magnetic field required to cause  $\mathbf{s}_k(\mathbf{R})$  to precess as the interface passes through  $\mathbf{R}$ .

<sup>12</sup> For closely related discussions, see Secs. I and VI of Ref. 3.

<sup>13</sup> C. Kittel and J. K. Galt, in *Solid State Physics*, edited by F. Seitz and D. Turnbull (Academic Press Inc., New York, 1956), Vol. 3.

In addition to the *effective* magnetic fields discussed thus far, the presence of a *real* magnetic field in a superconductor can be included in the equations of motion by replacing  $\nabla_{\mathbf{R}}$  by  $\nabla_{\mathbf{R}} - i(2e/\hbar c)\mathbf{A}(\mathbf{R})$ ,  $\mathbf{A}(\mathbf{R})$  being the magnetic vector potential at  $\mathbf{R}$ . This procedure, completely analogous to that used by Ginzburg and Landau,<sup>11</sup> takes account of the effect of the real magnetic field on the center-of-mass motion of the Cooper pairs, but does not properly describe magnetic effects on the internal motion of the Cooper pairs.

*Note added in proof.* By returning to the methods of Ref. 3, it can be shown that  $\nabla_{\mathbf{R}}$  should be replaced by  $\nabla_{\mathbf{R}} - i(2e/\hbar c)\mathbf{A}(\mathbf{R})$  only in the terms of  $\mathcal{H}_{\text{BCS}}$  containing  $s_{1k}$  and  $s_{2k}$ , not in those containing  $s_{3k}$ . (For the latter terms,  $\nabla_{\mathbf{R}}$  should remain unchanged.) Furthermore, only the so-called transverse portion of  $\mathbf{A}$  should be included in this replacement. Any longitudinal component of  $\mathbf{A}$ , corresponding to center-of-mass momentum of Cooper pairs, should be introduced as an additional kinetic energy in  $\mathcal{H}_{\text{BCS}}$ , having the form  $(1/4m)(2e\mathbf{A}_l/c)^2 \sum_k (\frac{1}{2} - s_{3k})$ .

### Spin-Wave Analysis of the Sublattice Magnetization Behavior of Antiferromagnetic and Ferromagnetic $\text{CrCl}_3$ †

ALBERT NARATH AND H. L. DAVIS\*

*Sandia Laboratory, Albuquerque, New Mexico*

(Received 3 August 1964)

The temperature and magnetic-field dependences of the sublattice magnetization in the hexagonal layer-type compound  $\text{CrCl}_3$  ( $T_N = 16.8^\circ\text{K}$ ) have been deduced from the  $^{53}\text{Cr}$  nuclear magnetic resonance (NMR) for  $0.4 \leq T \leq 8.1^\circ\text{K}$  and  $0 \leq H \leq 10$  kOe. The observed zero-field data can be accounted for over the whole temperature range by a renormalized spin-wave model based on isotropic ferromagnetic ( $J_T$ ) intralayer and antiferromagnetic ( $J_L$ ) interlayer exchange interactions in the presence of a weak effective anisotropy field ( $H_A$ ). Appropriate renormalized spin-wave dispersion relations are given for the four-sublattice antiferromagnetic (weak-field) and two-sublattice ferromagnetic (strong-field) equilibrium spin configurations. The validity of the two-dimensional approximation to these states is examined in detail for  $k_B T > 2|J_L|z_L S$  and  $|J_L| \ll J_T$ . It is shown that under these conditions the sublattice magnetizations for  $J_L < 0$  and  $J_L > 0$  are identical. The three-dimensional zero-field spin-wave fit gives  $J_T/k_B = 5.25^\circ\text{K}$ ,  $H_A(0) = 650$  Oe and a  $0^\circ\text{K}$ , zero-field  $^{53}\text{Cr}$  frequency  $\nu(0) = 63.318$  Mc/sec. Parallel magnetic susceptibilities calculated with these parameters in the range  $0.4 < T \leq 8.1^\circ\text{K}$  are in quantitative agreement with experimental values based on measured splittings of the  $^{53}\text{Cr}$  NMR in weak fields ( $H \leq 100$  Oe). The interlayer constant,  $J_L/k_B = -0.018^\circ\text{K}$ , used in the spin-wave calculations was obtained from single-crystal bulk magnetization measurements ( $\chi_1 = 9.9$  emu/mole for  $T \leq 4^\circ\text{K}$ ), corrected for demagnetizing effects. These measurements show that the net anisotropy in the ferromagnetic state (i.e.,  $H \geq 1.68$  kOe) is zero, presumably because of a cancellation of dipolar and single-ion contributions. The sublattice magnetization behavior in the ferromagnetic state appears to be strongly influenced by long-range dipolar interactions, as evidenced by significantly lower values of  $M(T, H)/M(0)$  for  $\mathbf{M} \parallel c$  than for  $\mathbf{M} \perp c$ .

#### I. INTRODUCTION

THE application of spin-wave theory to the measured sublattice magnetizations of  $\text{CrCl}_3$ <sup>1,2</sup> and  $\text{CrBr}_3$ <sup>3,4</sup> has provided considerable insight into the unusual magnetic properties of these isomorphous hex-

agonal, layer-type compounds. The exchange interactions in both cases are characterized by relatively

\* Present address: Bellcomm, Inc., 1100-17th N.W., Washington, D. C.

<sup>1</sup> A. Narath, *Phys. Rev. Letters* **7**, 410 (1961); A. Narath, *J. Appl. Phys.* **35**, 838 (1964).

<sup>2</sup> A. Narath, *Phys. Rev.* **131**, 1929 (1963).

<sup>3</sup> A. C. Gossard, V. Jaccarino, and J. P. Remeika, *Phys. Rev. Letters* **7**, 122 (1961).

<sup>4</sup> H. L. Davis and A. Narath, *Phys. Rev.* **134**, A433 (1964).

† This work was supported by the U. S. Atomic Energy Commission. Reproduction in whole or in part is permitted for any purpose of the U. S. Government.

strong ferromagnetic transverse couplings ( $J_T$ ) between nearest-neighbor  $\text{Cr}^{3+}$  ions in a given layer and much weaker longitudinal couplings ( $J_L$ ) between ions in adjacent layers. In  $\text{CrBr}_3$  the interlayer interaction is ferromagnetic ( $T_C=32.5^\circ\text{K}$ <sup>5</sup>), while in  $\text{CrCl}_3$  this interaction is antiferromagnetic ( $T_N=16.8^\circ\text{K}$ <sup>6</sup>). Because of the large ratio of intralayer to interlayer exchange energies, the spin-wave dispersion relations are highly anisotropic. The surfaces of constant energy in  $\mathbf{k}$  space are essentially prolate ellipsoids, for small  $\mathbf{k}$ , which encounter the zone boundary ( $k_L=\pm\pi/c_0$ ) at relatively small values of the spin-wave energy. The small energy associated with all spin-wave states which have wave vectors lying near  $[001]$  is expected to have a strong influence on the relevant thermodynamic quantities. This is a consequence of the large number of short-wavelength spin waves which are thermally excited even at low temperatures ( $T/T_C\ll 1$ ). Thus, deviations from the predictions of the continuum approximation to the Heisenberg exchange Hamiltonian are observed experimentally in  $\text{CrCl}_3$  and  $\text{CrBr}_3$  at temperatures corresponding to unusually small values of  $\Delta M/M_S$  (where  $\Delta M$  is the departure of the sublattice magnetization from its  $0^\circ\text{K}$  value,  $M_S$ ). These deviations are directly related to the large, thermal equilibrium populations of spin-wave states in the region of  $\mathbf{k}$  space  $k_L\gg k_T$  and can be attributed to two related effects: (1) zone boundary effects, and (2) spin-wave interactions.

Two previous studies, hereafter referred to as I<sup>2</sup> and II<sup>4</sup> bear on the present investigation: In I, precision measurements of  $\Delta M/M_S$  by means of the zero-field <sup>53</sup>Cr nuclear magnetic resonance (NMR) in antiferromagnetic  $\text{CrCl}_3$ , in the temperature range  $0.4\text{--}4.0^\circ\text{K}$ , were compared with predictions of a noninteracting spin-wave theory. It was shown that the interlayer exchange interaction in  $\text{CrCl}_3$  is sufficiently small to permit its replacement by an effective field. The resulting two-dimensional model represents an extreme example of the extent to which a zone boundary (in this case at  $k_L=\pm\pi/c_0$ ) can modify the temperature and magnetic field dependences of the observed sublattice magnetization. For example, for sufficiently small  $g\mu_B H_A/k_B T$  this model predicts a linear dependence of the sublattice magnetization on temperature, in good agreement with experiment. In II a similar treatment was carried out for ferromagnetic  $\text{CrBr}_3$ . Again zone boundary effects were found to be important at relatively low temperatures. Furthermore, the interpretation of the intermediate temperature data,  $4\text{--}20^\circ\text{K}$ , required the inclusion of spin-wave interaction effects in the analysis. A fit to the data, for the range  $1\text{--}20^\circ\text{K}$ , was achieved with a three-dimensional, renormalized spin-wave theory. The values of the exchange constants which were ob-

tained in I and II for  $\text{CrCl}_3$  and  $\text{CrBr}_3$ , respectively, are of interest because they are significantly larger than those which can be derived from the corresponding magnetic ordering temperatures, using the molecular field model.

The primary purpose of the present paper is the evaluation of spin-wave interaction effects in  $\text{CrCl}_3$  from the measured temperature dependence of the sublattice magnetization in the range  $0.4\text{--}8.1^\circ\text{K}$ . This study has enabled us to determine the intralayer exchange constant  $J_T$  with an accuracy comparable to that achieved previously in II for  $\text{CrBr}_3$ . In the course of this work we have also reexamined the bulk magnetization behavior of  $\text{CrCl}_3$  at  $4.0^\circ\text{K}$  and, from the resulting susceptibilities, deduced new values for the out-of-plane anisotropy and the interlayer exchange constant. In addition, we have measured the magnetic field dependence of the sublattice magnetization to  $\sim 10$  kOe in the range  $0.4\text{--}4.0^\circ\text{K}$ .

In Sec. II the relevant physical properties of  $\text{CrCl}_3$  are reviewed. The experimental techniques utilized in the present study are discussed in Sec. III. The results of our bulk magnetization measurements are presented in Sec. IV. In Sec. V the spin-wave theory appropriate for  $\text{CrCl}_3$  in the antiferromagnetic (low-field) and ferromagnetic (high-field) states is discussed. The appropriate three-dimensional spin-wave dispersion relations are given for the noninteracting and renormalized theories. The validity of the two-dimensional approximation is examined critically for the antiferromagnetic and ferromagnetic cases. In Sec. VI our results for the sublattice magnetization and parallel magnetic susceptibility, based on measurements of the <sup>53</sup>Cr NMR as a function of temperature and magnetic-field strength, are compared with our theoretical calculations. Finally, the results of our study are summarized and discussed in Sec. VII. The derivation of the spin-wave energies for the antiferromagnetic state is outlined in Appendix I for the noninteracting theory, and in Appendix II for the renormalized theory.

## II. REVIEW OF PHYSICAL PROPERTIES

Anhydrous  $\text{CrCl}_3$  has a structure composed of honeycomb layers of  $\text{Cr}^{3+}$  ions sandwiched between two closed-packed layers of  $\text{Cl}^-$  ions. It has been reported<sup>7</sup> to have a hexagonal unit cell of space group  $P3_112$  (or  $P3_212$ ) at room temperature. This assignment was recently shown to be incorrect.<sup>8</sup> Instead, crystals which are grown from the vapor by sublimation have monoclinic symmetry ( $C2/m$ ). At  $238\pm 4^\circ\text{K}$  unstrained specimens of  $\text{CrCl}_3$  undergo a polymorphic phase transition.<sup>8</sup> The low-temperature form has rhombohedral symmetry ( $R\bar{3}$ ) as shown in Fig. 1(a). This transformation is strongly affected by crystal imperfections. Powder specimens often transform incompletely on cooling, a

<sup>5</sup> From specific-heat measurements by L. D. Jennings and W. N. Hansen (private communication); magnetic susceptibility measurements give  $T_C\approx 37^\circ\text{K}$ , I. Tsubokawa, J. Phys. Soc. Japan 15, 1664 (1960).

<sup>6</sup> W. N. Hansen and M. Griffel, J. Chem. Phys. 28, 902 (1958).

<sup>7</sup> N. Wooster, Z. Krist. 74, 363 (1930).

<sup>8</sup> B. Morosin and A. Narath, J. Chem. Phys. 40, 1958 (1964).

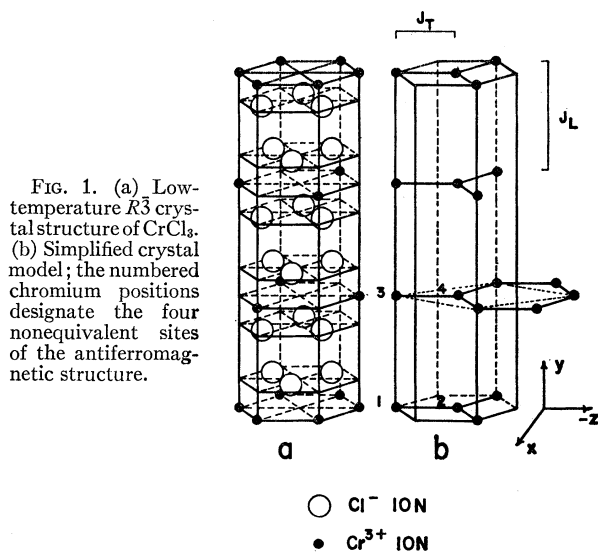


FIG. 1. (a) Low-temperature  $R\bar{3}$  crystal structure of  $\text{CrCl}_3$ . (b) Simplified crystal model; the numbered chromium positions designate the four nonequivalent sites of the antiferromagnetic structure.

large fraction remaining in the monoclinic form even at  $4^\circ\text{K}$ . For example, the extra  $^{53}\text{Cr}$  resonance reported in I is due to the monoclinic form of  $\text{CrCl}_3$ . We have established this by comparing intensity ratios of the two zero-field  $^{53}\text{Cr}$  resonances in the magnetically ordered state with intensity ratios of the  $^{35}\text{Cl}$  quadrupole resonances<sup>8</sup> in the paramagnetic state ( $76^\circ\text{K}$ ) in several powder specimens in which both structural forms were present at low temperatures. These comparisons revealed that the variation in the relative intensities of the two  $^{53}\text{Cr}$  signals in different samples followed the relative abundances of the monoclinic and rhombohedral forms, as determined from the intensities of the corresponding  $^{35}\text{Cl}$  resonances. The structural behavior of  $\text{CrCl}_3$  is identical to that of  $\text{CrBr}_3$ <sup>8,9</sup> although in the latter the polymorphic transition between the  $C2/m$  and  $R\bar{3}$  forms occurs above  $400^\circ\text{K}$ . Thus,  $\text{CrCl}_3$  and  $\text{CrBr}_3$  have isomorphous crystal structures in their respective magnetically ordered states. Since the  $R\bar{3}$  structure results from a solid-solid phase transformation involving a rearrangement in the stacking pattern of the chromium-halogen sandwiches, twinning along the  $c$  axis is found to be an inevitable occurrence.

A transition to a magnetically ordered state occurs in  $\text{CrCl}_3$  at  $16.8^\circ\text{K}$  as indicated by a  $\lambda$ -type specific-heat anomaly.<sup>6</sup> The magnetic structure has been determined by Cable *et al.*<sup>10</sup> using neutron diffraction techniques. The moments lie in (001) planes and form ferromagnetic layers which alternate in direction along the  $c$  axis. The magnetic unit cell contains 12  $\text{Cr}^{3+}$  ions. The antiferromagnetic interlayer coupling is quite weak compared to the ferromagnetic intralayer coupling. As a consequence,  $\text{CrCl}_3$  exhibits a strongly field-dependent

perpendicular magnetic susceptibility<sup>11</sup> and reaches ferromagnetic saturation in external magnetic fields of only  $\sim 2$  kOe. The magnetic anisotropies have also been found to be very small. The magnitude of the in-plane anisotropy field was estimated in I to be  $\sim 10$  Oe; the preferred direction of sublattice magnetization within the (001) planes, however, is not known. A vanishingly small out-of-plane anisotropy in the ferromagnetic state has been deduced by Dillon<sup>12</sup> from single-crystal ferromagnetic resonance experiments. The predominance of the intralayer exchange interaction among the various interactions involving the  $\text{Cr}^{3+}$  spins gives rise to the pronounced two-dimensional ferromagnetic character which was discussed in I.

### III. EXPERIMENTAL DETAILS

The  $\text{CrCl}_3$  samples used in the present study were derived from the polycrystalline sphere ( $\sim 7$ -mm diam) which was utilized in our earlier work.<sup>13</sup> This specimen was relatively strain free as evidenced by the fact that complete transformation to the rhombohedral form was always observed on cooling to  $4^\circ\text{K}$ . Furthermore, the  $\text{Cr}^{2+}$  content was judged to be low since the sample exhibited no detectable solubility in water.<sup>14</sup> Most of the  $^{53}\text{Cr}$  NMR measurements reported here were carried out on the original spherical specimen. It had the  $c$  axes of the individual plate-like grains oriented parallel throughout its volume; the basal plane orientations, however, were distributed essentially at random. In the course of our work the sphere accidentally cleaved into several fragments as a result of thermal shock. Subsequent bulk magnetization measurements were therefore carried out on thin single-crystal platelets which were cleaved from the fragments.

The  $^{53}\text{Cr}$  nuclear resonances were observed with a frequency swept push-pull FM marginal oscillator<sup>15</sup> as in our previous studies. Frequencies were determined with a digital counter. Magnetic field dependence measurements were made in a 12-in. electromagnet.

Temperatures between 0.4 and  $1.2^\circ\text{K}$  were attained with a recycling  $^3\text{He}$  cryostat described in I. The range  $1.2$ – $4.0^\circ\text{K}$  was covered by controlled pumping on a  $^4\text{He}$  bath. Above  $4.0^\circ\text{K}$  a vacuum-jacketed, copper heat-leak chamber was employed whose temperature was controlled manually by means of a heater. Temperature measurements below  $4.0^\circ\text{K}$  were based on the appropriate vapor pressure scales. Above  $4.0^\circ\text{K}$  the Curie law dependence of the magnetic susceptibility of chromium-methylammonium alum served as primary

<sup>11</sup> H. Bizette, C. Terrier, and A. Adam, *Compt. Rend.* **252**, 1571 (1961).

<sup>12</sup> J. F. Dillon, in *Magnetic and Electric Resonance and Relaxation*, edited by J. Smidt (Interscience Publishers, Inc., New York, 1963).

<sup>13</sup> This specimen was grown by L. R. Shiozawa, Clevite Corporation, Cleveland, Ohio.

<sup>14</sup> N. V. Sidgwick, *Chemical Elements and their Compounds* (Oxford University Press, London, 1950), Vol. 2, p. 1012.

<sup>15</sup> R. G. Shulman, *Phys. Rev.* **121**, 125 (1960).

<sup>9</sup> Å. Braekken, *Kgl. Norske Videnskab. Selskab. Forh* **5**, No. 11 (1932).

<sup>10</sup> J. W. Cable, M. K. Wilkinson, and E. O. Wollan, *Phys. Chem. Solids* **19**, 29 (1961).

standard; germanium resistance thermometers<sup>16</sup> served as secondary standards in this range. Our temperature measurements have an estimated maximum uncertainty of  $\pm 0.01^\circ\text{K}$  below  $4^\circ\text{K}$  and  $\pm 0.02^\circ\text{K}$  above  $4^\circ\text{K}$ .

The apparatus for measuring the bulk magnetization behavior of  $\text{CrCl}_3$  consisted of a  $\frac{1}{2}$  in. long, multiturn coil which was mounted rigidly at the center of a 15 kOe, 1.5-in.-diam bore, superconducting solenoid.<sup>17</sup> The emf induced when the sample was quickly withdrawn from the pick-up coil was measured with a critically damped ballistic galvanometer. The system was calibrated against the  $0^\circ\text{K}$  saturation moment ( $3\mu_B$ ) of  $\text{CrCl}_3$ .<sup>11</sup> The superconducting solenoid used in these experiments exhibited a constant negative trapped flux (at the center) of  $\simeq 100$  Oe, after field cycling, and our field measurements were corrected accordingly.

#### IV. BULK MAGNETIZATION MEASUREMENTS

The single-crystal magnetization behavior of  $\text{CrCl}_3$  has been studied previously by Bizette *et al.*<sup>11</sup> These authors, however, did not correct their data for demagnetizing effects and did not indicate the exact shape of their single-crystal specimen. Since  $\text{CrCl}_3$  has a very pronounced flake-like crystal habit when grown from the vapor, we made the assumption in I that their crystal was in the form of a very thin platelet with demagnetizing factors of  $4\pi$  and 0 parallel and perpendicular to the  $c$  axis, respectively. On the basis of this assumption we calculated an interlayer exchange field, at  $0^\circ\text{K}$ ,  $H_L = 1.45$  kOe and hence  $J_L z_L / k_B = -0.065^\circ\text{K}$ , where  $J_L$  is the interlayer exchange constant which couples to  $z_L$  nearest neighbors along the  $c$  axis, and  $k_B$  is Boltzmann's constant. Subsequent field-dependence measurements of the  $^{53}\text{Cr}$  NMR, described in Sec. VI of the present paper, showed that the interlayer exchange parameters of  $\text{CrCl}_3$  are considerably smaller than those given above. We concluded from these results that our assumption concerning the shape of the crystal used by Bizette *et al.* was in error. We have therefore performed a series of magnetization measurements on disk-shaped single-crystal specimens of varying thickness to diameter ratios. Demagnetizing factors were determined by comparing the field dependence of the  $^{53}\text{Cr}$  NMR in these crystals with that observed previously in the spherical specimen. The demagnetizing field in the sphere was taken to be  $H_{D.M.} = \frac{4}{3}\pi M_S = 1.42$  kOe at saturation ( $0^\circ\text{K}$ ). When our data were corrected in this way for shape anisotropy effects the different crystals yielded identical values for the true perpendicular magnetic susceptibility. The results for one of our crystals at  $4.0^\circ\text{K}$  are shown in Fig. 2. The most noteworthy feature of the data is the fact that shape effects account for *all* of the observed anisotropy. The true

perpendicular susceptibility is found to be

$$\chi_1(T \leq 4^\circ\text{K}) = 9.9 \text{ emu/mole}, \quad (4.1)$$

resulting from an antiferromagnetic exchange interaction given by

$$\begin{aligned} H_L &= 0.84 \pm 0.03 \text{ kOe}, \\ J_L z_L / k_B &= -0.037^\circ\text{K}. \end{aligned} \quad (4.2)$$

The lack of intrinsic magnetic anisotropy inferred from our static measurements is in complete accord with the ferromagnetic resonance observations by Dillon.<sup>12</sup> The isotropic character of the ferromagnetic state of  $\text{CrCl}_3$  must be the result of a fortuitous cancellation of dipolar and single-ion contributions to the net magnetic anisotropy. The presence of single-ion anisotropy was already inferred in I from the two-dimensional spin-wave analysis of sublattice magnetization data in the antiferromagnetic state. We have calculated the dipole field ( $H_D$ ) at the chromium sites for the ferromagnetic and antiferromagnetic states by direct summation (within a spherical volume) over point dipoles ( $3\mu_B$ ) lying in (001) planes. The calculated effective dipolar out-of-plane anisotropy fields ( $H_A = 3H_D$ ), (using  $225^\circ\text{K}$  lattice constants<sup>8</sup>), are given within an estimated accuracy of  $\pm 0.1\%$  by

$$\begin{aligned} H_A(\text{ferro}) &= 2.846 \text{ kOe}, \\ H_A(\text{antiferro}) &= 6.710 \text{ kOe}. \end{aligned} \quad (4.3)$$

From the results of these calculations and our magnetization measurements we conclude that the single-ion anisotropy field is equal to  $-2.85 \pm 0.10$  kOe. Hence, the net anisotropy field for the  $\mathbf{k} = 0$  out-of-plane mode in the antiferromagnetic state is calculated to be 3.86 kOe.

#### V. SPIN-WAVE THEORY

##### A. Spin Hamiltonian

The  $4F$  electronic ground state of the free  $\text{Cr}^{3+}$  ion retains only its fourfold spin degeneracy ( $S = \frac{3}{2}$ ) in the strong, predominantly octahedral crystal field of  $\text{CrCl}_3$ . The perturbations due to exchange, anisotropy, and any external magnetic field can be treated by the following model Hamiltonian:

$$\mathcal{H} = - \sum_{i'p, p'} J_{i'p, p'} \mathbf{S}_{i'p} \cdot \mathbf{S}_{i'p'} - g\mu_B \sum_{i,p} (H + H_{A,p}) S_{i,p}^z, \quad (5.1)$$

where  $i$  labels the cell and  $p (= 1, 2, 3, 4)$  designates the four nonequivalent sites in the approximate magnetic unit cell of Fig. 1(b). This simplification of the  $R\bar{3}$  lattice was first used by Gossard *et al.*<sup>3</sup> in connection with their early  $^{53}\text{Cr}$  NMR studies of ferromagnetic  $\text{CrBr}_3$ . The use of this lattice model is fully justified by the relatively small magnitude of the interlayer exchange interaction. In carrying out the sum over exchange-coupled pairs in (5.1) we have restricted ourselves to nearest-neighbor interactions within layers and

<sup>16</sup> Texas Instruments, Inc., Type 104-A.

<sup>17</sup> Westinghouse Electric Corporation, Cryogenic Systems Division.

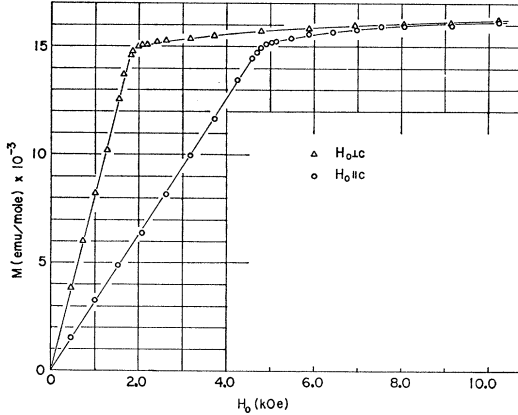


FIG. 2. Bulk magnetization behavior of  $\text{CrCl}_3$  at  $T=4.0^\circ\text{K}$  as a function of applied magnetic-field strength. The single crystal specimen was disk shaped and had a diameter to thickness ratio of 27. Demagnetizing factors are  $N(\parallel c)=0.85$ ,  $N(\perp c)=0.075$  where  $N=H_{D.M.}/4\pi M$ .

between layers, corresponding to exchange constants  $J_T \equiv J_{i'j',12} = J_{i'j',34}$  and  $J_L \equiv J_{i'j',13} = J_{i'j',24}$ , respectively. The applied magnetic field is denoted by  $H$ , and  $\mu_B$  is the Bohr magneton.

The most serious approximation in (5.1) is probably the representation of the anisotropic interactions by an effective anisotropy field  $H_A = |H_{A,p}|$ . The normal-mode spectrum of (5.1) for  $J_L < 0$  and  $H=0$  is doubly degenerate with an energy gap at  $\mathbf{k}=0$  for the acoustical branch equal to  $g\mu_B[2H_A H_L + H_A^2]^{1/2}$ . This behavior is characteristic of an antiferromagnetic lattice<sup>18</sup> in which the directions of sublattice magnetization coincide with the principal direction of a uniaxial anisotropy. The anisotropy in  $\text{CrCl}_3$  is nearly uniaxial; its symmetry axis, however, lies normal to an easy plane. Yoshimori<sup>19</sup> has recently examined this case for a single-ion uniaxial anisotropy of the form  $D(S^y)^2$ . He has evaluated the corresponding normal modes to order  $k_T^2$ . The degeneracy of the spectrum is no longer present, resulting in two  $\mathbf{k}=0$  modes with energies 0 and  $[6g\mu_B D H_L]^{1/2}$ . With increasing  $\mathbf{k}_T$ , however, the difference between the normal modes of (5.1) and those derived by Yoshimori becomes vanishingly small. For this reason the thermodynamic properties calculated on the basis of the two models are expected to differ significantly only at temperatures approaching the gap temperature. From the results of Sec. IV we obtain

$$[6g\mu_B D H_L]^{1/2}/k_B = 0.34^\circ\text{K}. \quad (5.2)$$

Our measurements of the  $\text{CrCl}_3$  sublattice magnetization were restricted to temperatures above  $\sim 0.4^\circ\text{K}$ . We have therefore used the approximate Hamiltonian (5.1) because of the great simplification which results in the subsequent analysis. Furthermore, it should be

remarked that even Yoshimori's small- $\mathbf{k}_T$  spectrum is only an approximation to the true spin-wave modes in  $\text{CrCl}_3$ . This follows from the fact that the net out-of-plane anisotropy in  $\text{CrCl}_3$  is largely of dipolar origin and hence can be accurately approximated by a single-ion term only for excitations near  $\mathbf{k}=0$ . We have therefore treated the "average" effective anisotropy field  $H_A$  as an adjustable parameter. In view of our measurements of the in-plane and out-of-plane anisotropies it is obvious that a physically realistic fit of the theory to the sublattice magnetization data requires that the magnitude of the anisotropy obtained from such a fit lie in the range  $10 < H_A < 3860$  Oe.

## B. Noninteracting Spin Waves

In the following we examine the eigenvalue spectrum of (5.1) for both antiferromagnetic and ferromagnetic equilibrium spin arrangements. In addition, we re-examine the validity of the two-dimensional approximation to these modes. The antiferromagnetic solutions which we consider here apply to  $\text{CrCl}_3$  in the limit of zero external field, or in the presence of a parallel external field whose magnitude does not exceed the spin-flop field<sup>2</sup> (i.e.,  $H \lesssim 100$  Oe). The ferromagnetic solutions apply for fields sufficiently strong to produce technical saturation of the net magnetization ( $H \gtrsim 1.68$  kOe). At sufficiently low temperatures the eigenvalues of (5.1) are given by the linear spin-wave approximation of Holstein and Primakoff.<sup>20</sup>

### 1. Antiferromagnetic State

The transformations which diagonalize  $\mathcal{H}$  are given in Appendix I. The total energy of the system is found to be

$$\begin{aligned} \mathcal{H}_0 &= E_0 + \sum_{\mathbf{k}t} \omega_{\mathbf{k}t} (n_{\mathbf{k}t} + \frac{1}{2}); \quad n_{\mathbf{k}t} = 0, 1, 2, \dots, \\ E_0 &= -4N[g\mu_B(H_A + H)(S + \frac{1}{2}) \\ &\quad + S(S+1)(J_T z_T - J_L z_L)], \end{aligned} \quad (5.3)$$

where  $N$  denotes the number of cells in the system and  $g$  is the spectroscopic splitting factor ( $g=2.00$ ). Also  $\mathbf{k}$  is the wave vector of the normal modes and  $t(=1, 2, 3, 4)$  is the branch index. The spin-wave energies are given by

$$\omega_{\mathbf{k}t} = \omega_{(e)\mathbf{k}t} + R_t g\mu_B H, \quad (5.4)$$

where

$$\begin{aligned} R_t &= +1 \quad \text{for } t=1, 2 \\ &= -1 \quad \text{for } t=3, 4, \end{aligned}$$

with

$$\begin{aligned} \omega_{(e)\mathbf{k}t} &= [(\omega_{(0)\mathbf{k}t})^2 - (2J_L z_L S \gamma_{(L)\mathbf{k}})^2]^{1/2} \\ \omega_{(0)\mathbf{k}t} &= 2J_T z_T S [1 - (-1)^t |\gamma_{(T)\mathbf{k}}|] \\ &\quad - 2J_L z_L S + g\mu_B H_A, \end{aligned} \quad (5.5)$$

where

$$|\gamma_{(T)\mathbf{k}}| = [\gamma_{(T)\mathbf{k}} \gamma_{(T)-\mathbf{k}}]^{1/2}.$$

<sup>18</sup> J. Van Kranendonk and J. H. Van Vleck, Rev. Mod. Phys. **30**, 1 (1958).

<sup>19</sup> A. Yoshimori, Phys. Rev. **130**, 1312 (1963).

<sup>20</sup> T. Holstein and H. Primakoff, Phys. Rev. **58**, 1098 (1940).

Also

$$\begin{aligned}\gamma_{(T)\mathbf{k}} &= z_T^{-1} \sum_m \exp(-i\mathbf{k}_T \cdot \mathbf{r}_m), \quad (z_T=3), \\ \gamma_{(L)\mathbf{k}} &= z_L^{-1} \sum_n \exp(-i\mathbf{k}_L \cdot \mathbf{r}_n), \quad (z_L=2),\end{aligned}\quad (5.6)$$

where  $\mathbf{r}_m$  and  $\mathbf{r}_n$  denote vectors connecting a given  $\text{Cr}^{3+}$  lattice point to its nearest  $\text{Cr}^{3+}$  neighbors within the layer and in the two adjacent layers, respectively. It is seen that for sufficiently large  $\mathbf{k}_T$  the modes (5.4) are essentially identical to the two-dimensional modes

$$\omega'_{\mathbf{k}t} = \omega_{(0)\mathbf{k}t} + g\mu_B H, \quad (5.7)$$

provided that  $|J_L| \ll J_T$ . This similarity has already been discussed in I. The temperature dependence of the sublattice magnetization can be readily calculated from the dispersion relation (5.4) and a knowledge of the eigenvectors of  $\mathcal{H}$  (Appendix I).

$$\begin{aligned}\frac{M(T)_p}{M_S} &= 1 - \frac{\Delta M(T)_p}{M_{S,p}} = \left\{ 1 + \frac{1}{2S} - \frac{1}{4NS} \right. \\ &\times \sum_{\mathbf{k}t} \left[ \left( \langle n_{\mathbf{k}t} \rangle + \frac{1}{2} \right) \left( \frac{\omega_{(0)\mathbf{k}t}}{\omega_{(e)\mathbf{k}t}} + R_p R_t \right) \right] \Big\} \\ &R_p = +1 \quad \text{for } p=1, 2 \\ &R_p = -1 \quad \text{for } p=3, 4,\end{aligned}\quad (5.8)$$

where  $M(T)_p$  is the magnetization of the  $p$ th sublattice and  $M_{S,p}$  is the corresponding saturation magnetization. Since the excitations of the system are bosons, the statistical average of  $n_{\mathbf{k}t}$  is given by

$$\langle n_{\mathbf{k}t} \rangle = [\exp(\omega_{\mathbf{k}t}/k_B T) - 1]^{-1}. \quad (5.9)$$

The magnetic-field dependence of the magnetization of a sublattice is given by

$$\begin{aligned}\frac{\partial M(T)_p}{\partial H} &= (g\mu_B)^2 (4k_B T N)^{-1} \sum_{\mathbf{k}t} \left\{ \left[ 1 + \frac{R_p R_t \omega_{(0)\mathbf{k}t}}{\omega_{(e)\mathbf{k}t}} \right] \right. \\ &\times \left. \left[ \frac{\exp(\omega_{\mathbf{k}t}/k_B T)}{[\exp(\omega_{\mathbf{k}t}/k_B T) - 1]^2} \right] \right\},\end{aligned}\quad (5.10)$$

which leads to the standard spin-wave prediction<sup>21</sup> for the parallel magnetic susceptibility

$$\begin{aligned}\chi_{||} &= \sum_p \frac{\partial M(T)_p}{\partial H} = (g\mu_B)^2 (k_B T N)^{-1} \\ &\times \sum_{\mathbf{k}t} \left\{ \frac{\exp(\omega_{\mathbf{k}t}/k_B T)}{[\exp(\omega_{\mathbf{k}t}/k_B T) - 1]^2} \right\}.\end{aligned}\quad (5.11)$$

## 2. Ferromagnetic State

In an external magnetic field of sufficient strength to produce a parallel alignment of the sublattices, the

<sup>21</sup> T. Nagamiya, K. Yosida, and R. Kubo, *Advan. Phys.* **4** (1955).

appropriate spin-wave states of (5.1) are identical to those derived previously for ferromagnetic  $\text{CrBr}_3$ .<sup>3,4</sup> The necessary transformations are given in II. There are now only two sublattices and hence two spin-wave branches ( $t=1, 2$ ). The total energy is given by

$$\mathcal{H}_0 = E_0 + \sum_{\mathbf{k}t} \omega_{\mathbf{k}t} n_{\mathbf{k}t}, \quad (5.12)$$

$$E_0 = -2N[J_T z_T S^2 + J_L z_L S^2 + g\mu_B S(H_A + H)],$$

with spin-wave energies

$$\omega_{\mathbf{k}t} = \omega_{(e)\mathbf{k}t} + g\mu_B H. \quad (5.13)$$

In this case

$$\begin{aligned}\omega_{(e)\mathbf{k}t} &= \omega_{(0)\mathbf{k}t} - 2J_L z_L S \gamma_{(L)\mathbf{k}} \\ \omega_{(0)\mathbf{k}t} &= 2J_T z_T S [1 - (-1)^t |\gamma_{(T)\mathbf{k}}|] \\ &\quad + 2J_L z_L S + g\mu_B H_A,\end{aligned}\quad (5.14)$$

where  $\omega_{(0)\mathbf{k}t}$  differs from the corresponding antiferromagnetic expression only in the sign of the  $J_L$  term. The sublattice magnetization is given by

$$\frac{M(T)}{M_S} = \frac{M(T)}{M(0)} = \left[ 1 - \frac{1}{2NS} \sum_{\mathbf{k}t} \langle n_{\mathbf{k}t} \rangle \right]. \quad (5.15)$$

## 3. Two-Dimensional Approximation

The two-dimensional approximation to the spin-wave states of (5.1) consists of neglecting the  $\mathbf{k}_L$  dependence of the corresponding energies. The validity of this approximation depends on the condition  $|J_L| \ll J_T$  which, as shown in I, appears to be well satisfied in  $\text{CrCl}_3$ . The error which is introduced in the calculated sublattice magnetization by the two-dimensional approximation can be evaluated as follows. We assume a zero external field,  $H=0$ . For the antiferromagnetic spin configuration ( $J_L < 0$ ) the difference between the thermal equilibrium magnetizations calculated on the basis of the three- and two-dimensional models is then given, according to (5.5), (5.8), and (5.9), by

$$\begin{aligned}\mathcal{E} &= \left( \frac{\Delta M(T)}{M_S} \right)_3 - \left( \frac{\Delta M(T)}{M_S} \right)_2 \\ &= (4S)^{-1} (2\pi)^{-3} V_0 \sum_t \int \int \int d\mathbf{k} \{ \omega_{(0)\mathbf{k}t} \\ &\quad \times (\omega_{(e)\mathbf{k}t})^{-1} [\exp(\omega_{(e)\mathbf{k}t}/k_B T) - 1]^{-1} \\ &\quad - [\exp(\omega_{(0)\mathbf{k}t}/k_B T) - 1]^{-1} \},\end{aligned}\quad (5.16)$$

where  $V_0$  is the volume of the unit cell. The sum over spin-wave states has been replaced in the usual way by an integration over the first Brillouin zone. We have also ignored the zero-point reduction of the sublattice magnetization since this is negligible<sup>2</sup> in the present case. Since  $\omega_{(e)\mathbf{k}t}$  and  $\omega_{(0)\mathbf{k}t}$  are significantly different only for small  $\mathbf{k}_T$ , the integrand in (5.16) differs signifi-

cantly from zero only for small values of the spin-wave energy. We shall restrict our discussion to temperatures such that the important contributions to  $\mathcal{E}$  come from states for which  $\omega/k_B T < 1$ . In practice this implies  $k_B T > 2|J_L|z_L S$ , in addition to our previous assumption  $|J_L| \ll J_T$ . The expression (5.16) can then be simplified by performing a linear expansion of the exponentials.

$$\mathcal{E} = (4S)^{-1} (2\pi)^{-3} V_0 k_B T \sum_t \int \int \int d\mathbf{k} (\omega_{(0)\mathbf{k}t})^{-1} \times \{ [1 - (E_L \gamma_{(L)\mathbf{k}} / \omega_{(0)\mathbf{k}t})^2]^{-1} - 1 \}, \quad (5.17)$$

where  $E_L = -2J_L z_L S$ . The integration over  $\mathbf{k}_L$  can now be performed exactly, giving

$$\mathcal{E} = (4S)^{-1} (2\pi)^{-2} V_0 c_0^{-1} k_B T \sum_t \int \int d\mathbf{k}_T (\omega_{(0)\mathbf{k}t})^{-1} \times \{ [1 - (E_L / \omega_{(0)\mathbf{k}t})^2]^{-1/2} - 1 \}. \quad (5.18)$$

The integration over  $\mathbf{k}_T$  can be simplified by taking the long-wave limit for the acoustical branches ( $t=2, 4$ ) of  $\omega_{(0)\mathbf{k}t}$  and ignoring the two upper branches.

$$\omega_{(0)\mathbf{k}(2,4)} \approx \frac{1}{2} J_T S k_T^2 a_0^2 + E_L + E_A, \quad (5.19)$$

where  $a_0$  is the basal plane lattice constant and  $E_A = g\mu_B H_A$ . Because of the rapid convergence of the integral in (5.18) the limit of integration can be taken as infinity. Finally we obtain

$$\mathcal{E} = 3^{1/2} k_B T (8\pi S^2 J_T)^{-1} \times \ln \{ 2 [1 + [1 - E_L^2 (E_L + E_A)^{-2}]^{1/2}]^{-1} \}. \quad (5.20)$$

The error  $\mathcal{E}$  clearly vanishes when  $E_L = 0$  since the two-dimensional model is then exact. For any given  $E_L$  the error is maximum when  $E_A = 0$ ; thus

$$\mathcal{E}(\text{max}) = 3^{1/2} k_B T (8\pi S^2 J_T)^{-1} \ln 2. \quad (5.21)$$

It is useful to evaluate the error relative to the reduction in sublattice magnetization ( $\Delta M(T)/M_S$ ). Calculating  $\Delta M(T)$  in the long wave limit<sup>1,2</sup> we obtain

$$\mathcal{E} \times \left( \frac{\Delta M(T)}{M_S} \right)^{-1} = \left\{ \ln \left[ \frac{2(1+\alpha)}{(1+\alpha) + (\alpha^2 + 2\alpha)^{1/2}} \right] \right\} \left\{ \ln \left[ \frac{2(1+\alpha)}{[(1+\alpha) + (\alpha^2 + 2\alpha)^{1/2}] [1 - \exp[-\beta(1+\alpha)]]} \right] \right\}^{-1}, \quad (5.22)$$

where

$$\alpha = E_A / E_L, \\ \beta = E_L / k_B T.$$

The error function (5.22) has been plotted in Fig. 3 for several representative values of  $\alpha$ . The results of our analysis show that the two-dimensional model introduces errors of less than 10% in the calculated values of  $\Delta M(T)$  for CrCl<sub>3</sub> based on the exchange and anisotropy parameters determined in I.

We now examine the validity of the two-dimensional model when the interlayer exchange coupling is ferro-

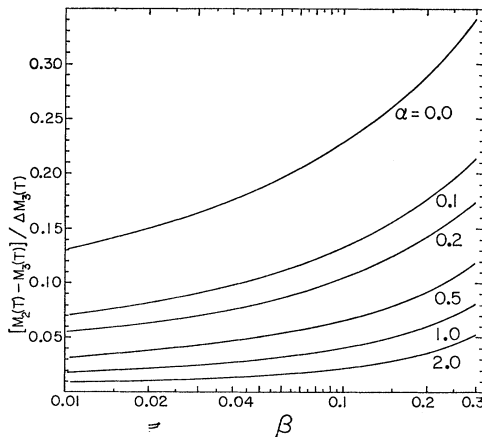


FIG. 3. Plot of the relative error in  $\Delta M(T)M_S$ , which is introduced by the two-dimensional spin-wave approximation, as a function of  $\beta (= E_L/k_B T)$  for several values of  $\alpha (= E_A/E_L)$ .

magnetic ( $J_L > 0$ ). Using (5.13), (5.14), and (5.15) we find

$$\mathcal{E} = (2S)^{-1} (2\pi)^{-3} V_0 \times \sum_t \int \int \int d\mathbf{k} \{ [\exp(\omega_{(e)\mathbf{k}t} / k_B T) - 1]^{-1} - [\exp(\omega_{(0)\mathbf{k}t} / k_B T) - 1]^{-1} \}. \quad (5.23)$$

Proceeding as before, we obtain

$$\mathcal{E} = (2S)^{-1} (2\pi)^{-3} V_0 k_B T \sum_t \int \int \int d\mathbf{k} (\omega_{(0)\mathbf{k}t})^{-1} \times \{ [1 - (E_L \gamma_{(L)\mathbf{k}} / \omega_{(0)\mathbf{k}t})^2]^{-1} - 1 \}, \quad (5.24)$$

where  $E_L = 2J_L z_L S$ . Then

$$\mathcal{E} = (2S)^{-1} (2\pi)^{-2} V_0 c_0^{-1} k_B T \sum_t \int \int d\mathbf{k}_T (\omega_{(0)\mathbf{k}t})^{-1} \times \{ [1 - (E_L / \omega_{(0)\mathbf{k}t})^2]^{-1/2} - 1 \}. \quad (5.25)$$

Since there are only two branches ( $t=1, 2$ ) in the ferromagnetic case, it follows that (5.25) is identical to (5.18). Consequently, the error introduced by the two-dimensional model is identical for the ferromagnetic and antiferromagnetic cases. This shows that for given magnitudes of  $J_T$ ,  $J_L$ , and  $H_A$  the low-temperature sublattice magnetizations are independent of the sign of  $J_L$ , provided that  $|J_L| \ll J_T$ . This conclusion differs from

that reached by Shore<sup>22</sup> who recently considered the problem of exchange inversion<sup>23</sup> in planar, tetragonal magnetic systems. By comparing leading terms in the appropriate low-temperature power-series expansions of  $\Delta M(T)$  for  $J_L > 0$  and  $J_L < 0$ , he concluded that the sublattice magnetization in the antiferromagnetic state is slightly larger at a given temperature than the magnetization in the ferromagnetic state. This finite difference in the calculated magnetization behaviors resulted from the invalid assumption  $\omega_{(0)kt}/\omega_{(e)kt} = 1$  in the expression for the antiferromagnetic sublattice magnetization (5.8). This factor is sufficiently close to unity for most modes to make the predicted zero-point reduction of the sublattice magnetization negligibly small. However, whereas zero-point effects are determined by an unweighted average of  $[1 - (\omega_{(0)kt}/\omega_{(e)kt})]$  over all spin-wave states, the thermal excitations depend on averages in which contributions from various states are weighted by the Bose distribution function. In other words, the reduction of the magnetization due to thermal excitations is influenced much more strongly by the low-frequency modes than is the case for the zero-point reduction. Since the deviation of  $\omega_{(0)kt}/\omega_{(e)kt}$  from unity becomes most pronounced for the low-frequency modes, the assumption  $\omega_{(0)kt}/\omega_{(e)kt} = 1$  is not justified for an accurate calculation of the magnetization. We have shown that if this factor is correctly included in such a calculation, the difference between the predicted ferromagnetic and antiferromagnetic sublattice magnetizations vanishes. Hence, if an exchange inversion occurs in a planar system in which  $|J_L| \ll J_T$  one would not expect a discontinuous change in the sublattice magnetization unless  $|J_L|$  changes at the transition.

### C. Renormalized Spin Waves

At sufficiently low temperatures the spin-wave states discussed in the previous section are known to be good approximations<sup>24</sup> to the true eigenstates of (5.1). However, when temperatures are reached at which appreciable populations of spin waves (particularly those of short wavelength) are thermally excited, interaction terms which were not included in  $\mathcal{H}_0$  become important. It has been shown<sup>4,25,26</sup> that the usefulness of the quasiparticle approach in the presence of interactions can be extended up to temperatures of at least  $T/T_e \approx 0.5$  by renormalization of the energies. In this way several accurate fits of spin-wave theory to sublattice magnetization data have been obtained, notably for antiferromagnetic<sup>26</sup>  $\text{MnF}_2$  and ferromagnetic<sup>4</sup>  $\text{CrBr}_3$ . The renormalization of the spin-wave energies is accom-

plished by taking

$$\mathcal{H} = \mathcal{H}_0 + \mathcal{H}_{1d}, \quad (5.26)$$

where  $\mathcal{H}_{1d}$  denotes contributions from quartic terms in  $\mathcal{H}$  which are diagonal in the  $n_{kt}$  representation. In this approximation the spin-wave contribution to the energy is given by  $\sum_{kt} \epsilon_{kt} n_{kt}$  where  $\epsilon_{kt}$  are the renormalized spin-wave energies which are now a function of the temperature. Also

$$\langle n_{kt} \rangle = [\exp(\epsilon_{kt}/k_B T) - 1]^{-1}, \quad (5.27)$$

since the excitations are still pure bosons. We now consider the explicit form of the renormalized energies for the two limiting spin configurations.

#### 1. Antiferromagnetic State

The derivation of the renormalized modes for the case  $H = 0$  is indicated in Appendix II. The zero-field energies are found to be

$$\begin{aligned} \epsilon_{(e)kt} = \omega_{(e)kt} + \{ & 2J_T z_T S \omega_{(0)kt} \\ & \times (\omega_{(e)kt})^{-1} [1 - (-1)^t |\gamma_{(T)k}|] (\xi_T - 1) \\ & - 2J_L z_L S (\omega_{(e)kt})^{-1} \\ & \times [2J_L z_L S (\gamma_{(L)k})^2 + \omega_{(0)kt}] (\xi_L - 1) \}. \end{aligned} \quad (5.28)$$

The renormalization coefficients  $\xi$  are independent of  $\mathbf{k}$  and  $t$  and are given by

$$\begin{aligned} \xi_T = 1 - (4SN)^{-1} \sum_{kt} \langle n_{kt} \rangle \{ & \omega_{(0)kt} \\ & \times (\omega_{(e)kt})^{-1} [1 - (-1)^t |\gamma_{(T)k}|] \}, \\ \xi_L = 1 - (4SN)^{-1} \sum_{kt} \langle n_{kt} \rangle \{ & (\omega_{(e)kt})^{-1} \\ & \times [2J_L z_L S (\gamma_{(L)k})^2 + \omega_{(0)kt}] \}. \end{aligned} \quad (5.29)$$

#### 2. Ferromagnetic State

As was the case for the noninteracting modes, the form of the renormalized modes for the high-field, ferromagnetic state of  $\text{CrCl}_3$  is identical to that derived for  $\text{CrBr}_3$  in II. Using the present notation we have

$$\begin{aligned} \epsilon_{kt} = \epsilon_{(e)kt} + g\mu_B H, \\ \epsilon_{(e)kt} = \omega_{(e)kt} + \{ 2J_T z_T S [1 - (-1)^t |\gamma_{(T)k}|] \\ \times (\xi_T - 1) + 2J_L z_L S [1 - \gamma_{(L)k}] (\xi_L - 1) \}, \end{aligned} \quad (5.30)$$

with

$$\begin{aligned} \xi_T = 1 - (2SN)^{-1} \sum_{kt} \langle n_{kt} \rangle [1 - (-1)^t |\gamma_{(T)k}|], \\ \xi_L = 1 - (2SN)^{-1} \sum_{kt} \langle n_{kt} \rangle [1 - \gamma_{(L)k}]. \end{aligned} \quad (5.31)$$

In the ferromagnetic case the expression (5.30) can be simplified, giving

$$\begin{aligned} \epsilon_{kt} = 2J_T z_T S \xi_T [1 - (-1)^t |\gamma_{(T)k}|] \\ + 2J_L z_L S \xi_L [1 - \gamma_{(L)k}] + g\mu_B (H_A + H). \end{aligned} \quad (5.32)$$

<sup>22</sup> H. B. Shore, Phys. Rev. **131**, 2496 (1963).

<sup>23</sup> C. Kittel, Phys. Rev. **120**, 335 (1960).

<sup>24</sup> L. R. Walker, *Magnetism* (Academic Press Inc., New York, 1963), Vol. 1, Chap. 8.

<sup>25</sup> M. Bloch, Phys. Rev. Letters **9**, 286 (1962).

<sup>26</sup> G. G. Low, Proc. Phys. Soc. (London) **82**, 992 (1963).



### 3. Temperature Dependence of $\xi$

The corrections to the spin-wave energies given above are similar to those obtained by other authors for cubic lattices. Our results differ in detail because of the more complex magnetic lattice which we have treated here. In the limit  $J_T \rightarrow 0$  the implicit equations (5.28), (5.29) are equivalent to Oguchi's<sup>27</sup> result for the cubic two-sublattice antiferromagnet. In the limit  $J_L \rightarrow 0$  our expressions are equivalent to Bloch's<sup>25</sup> result for the cubic ferromagnet. At low temperatures the corrections to the spin-wave energies are essentially proportional to the mean spin-wave energy<sup>28</sup> and are thus quite small. Since  $|J_L| \ll J_T$  one expects  $\xi_L$  to decrease much more rapidly than  $\xi_T$ . Indeed, an inspection of the expressions (5.29) and (5.31) shows that for temperatures which exceed  $\sim 2|J_L|z_L S/k_B$  the longitudinal renormalization constant approaches the molecular field value

$$\xi_L \approx M(T)/M(0). \quad (5.33)$$

This follows from the fact that  $\langle n_{kt} \rangle$  becomes essentially independent of  $\mathbf{k}_L$  at these temperatures (i.e., the two-dimensional approximation holds) and hence the  $\gamma_{(L)\mathbf{k}}$  term can be averaged separately to unity. Thus in planar systems such as CrCl<sub>3</sub> and CrBr<sub>3</sub> a significant reduction of the longitudinal exchange interaction is expected at temperatures which are *small* compared to the ordering temperature. Therefore, these systems provide a unique opportunity for the observation of large dynamical interaction effects between spin waves, in the complete absence of significant kinematic<sup>29</sup> effects. The latter is a consequence of the relatively small number of spin waves which exist in thermal equilibrium at these low temperatures.

## VI. SUBLATTICE MAGNETIZATION MEASUREMENTS

In this section we report on measurements of the temperature and magnetic field dependences of the CrCl<sub>3</sub> sublattice magnetization and their interpretation by the spin-wave theory developed in the preceding section. Our measurements are based on the observed resonance frequencies of the <sup>53</sup>Cr NMR and thus provide accurate values of the *relative* sublattice magnetization. In relating the measured hyperfine fields to  $\langle S_p^z \rangle$  we have assumed that the hyperfine coupling constant is independent of temperature in the range  $T \lesssim 8^\circ\text{K}$ .

### A. Low-Field Experiments

Measurements of the zero-field <sup>53</sup>Cr NMR in the range  $0.4 \leq T \leq 4.0^\circ\text{K}$  have been reported previously in I. Between 2 and  $4^\circ\text{K}$ , these results confirmed the nearly

linear behavior of  $\Delta M(T)/M(0)$  predicted for a two-dimensional ferromagnet with weak anisotropy. We have now extended these measurements to  $\sim 8^\circ\text{K}$  ( $T/T_N \approx 0.5$ ). The new results show that the slope of  $\Delta M(T)$  versus  $T$  increases markedly above  $4^\circ\text{K}$ , indicative of spin-wave interaction effects. In fact, it is not possible to obtain a fit of the noninteracting spin-wave model (5.5), (5.8) to our data for any choice of the adjustable parameters  $J_T$  and  $H_A$ . We have therefore applied the renormalized theory by using the renormalized energies (5.28) in (5.8). Zero-point effects were ignored because of their negligible contribution to  $\Delta M(T)$ . The effective anisotropy  $H_A$  was given an explicit temperature dependence, according to the spin-wave result<sup>30</sup> for dipolar anisotropy

$$H_A(T) = H_A(0)[M(T)/M(0)]^2. \quad (6.1)$$

The  $[M(T)]^2$  dependence in (6.1) is rigorous in the low-temperature limit (i.e., when all spins which contribute significantly to the dipolar anisotropy are completely correlated). With increasing temperature, the thermal excitation of short-wavelength spin waves decreases the spacial correlation and hence the  $[M(T)]$  dependence given by the molecular field approximation gradually takes over. In the antiferromagnetic state of CrCl<sub>3</sub> the dipolar contribution to the spin-wave energies, for most of  $\mathbf{k}$  space, arises primarily from intralayer spin pairs. For example, the intralayer and interlayer contributions to the static dipole field at a chromium site are calculated to be +2254 and  $-17$  Oe, respectively. Because of the large intralayer exchange energy, however, the correlation length within a given layer remains quite long even at the highest temperature of our experiments. Hence, the low-temperature form, (6.1), is expected to approximate very well the true temperature dependence of the average, effective anisotropy field  $H_A(T)$ . The relative sublattice magnetization in (6.1) was taken from our NMR measurements. The values of  $J_T$  and  $H_A$  obtained in I served as a guide in achieving a fit of the theory to experiment. The calculation of  $\Delta M(T)$  for a given choice of parameters was carried out by obtaining a self-consistent numerical solution for the implicit equations for  $\xi_T$ ,  $\xi_L$ , and  $\langle n_{kt} \rangle$  according to (5.27), (5.28), and (5.29). The calculations were performed on a CDC-1604 digital computer, taking full account of the finite extent of the first Brillouin zone. Both acoustical and optical spin-wave branches were included. Thus, the results of our calculations are numerically "exact," assuring that any errors result from the theory itself and not its application. The numerical methods for obtaining an iterative solution for the temperature dependent renormalization coefficients  $\xi_T$  and  $\xi_L$  were similar to those described in II. Computer time was minimized by restricting the initial

<sup>27</sup> T. Oguchi, Phys. Rev. **117**, 117 (1960).

<sup>28</sup> F. Keffer and R. Loudon, Suppl. J. Appl. Phys. **32**, 2S (1961).

<sup>29</sup> F. J. Dyson, Phys. Rev. **102**, 1217, 1230 (1956).

<sup>30</sup> J. Kanamori, *Magnetism* (Academic Press Inc., New York, 1963), Vol. 1, Chap. 4.

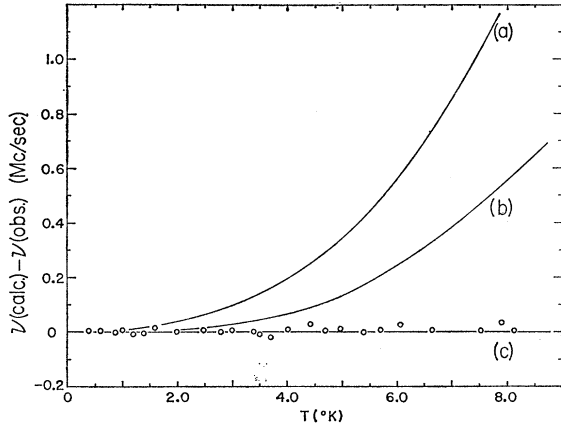


FIG. 4. Plot of  $\nu_{\text{calc.}} - \nu_{\text{obs.}}$  for the three-dimensional spin-wave model with  $J_T/k_B = 5.25^\circ\text{K}$ ,  $J_L/k_B = -0.018^\circ\text{K}$ ,  $H_A(0) = 650$  Oe, and  $\nu(0) = 63.318$  Mc/sec: (a) Noninteracting spin-wave model with temperature-independent  $H_A$ . (b) Noninteracting spin-wave model with  $H_A(T) = H_A(0)[M(T)/M(0)]^2$ . (c) Renormalized spin-wave model with  $H_A(T) = H_A(0)[M(T)/M(0)]^2$ .

calculations to only two temperatures (4 and 8°K). Aided by the earlier spin-wave fits, correct values for  $J_T$  and  $H_A(0)$  were quickly determined. Because of the sensitivity of the fit to slight changes in the parameters, subsequent calculations for other temperatures required no further adjustment in these parameters. We find that the three-dimensional renormalized theory gives

$$\begin{aligned} J_T/k_B &= 5.25 \pm 0.05^\circ\text{K}, \\ H_A(0) &= 650 \mp 50 \text{ Oe}, \\ \nu(0) &= 63.318 \text{ Mc/sec}, \end{aligned} \quad (6.2)$$

where we have used  $J_L/k_B = -0.018^\circ\text{K}$  from our susceptibility measurements. Table I summarizes these zero-field results. The listed NMR frequencies correspond to the central ( $+\frac{1}{2} \leftrightarrow -\frac{1}{2}$ ) transition of the  $^{53}\text{Cr}$  ( $I = \frac{3}{2}$ ) quadrupole triplet. In order to take advantage of the weak-field enhancement<sup>2</sup> of the  $^{53}\text{Cr}$  NMR, the resonances were detected in external fields of 10–50 Oe and the measured frequencies extrapolated to zero field. The resulting rms deviation from the theory of 13 kc/sec lies within our estimated experimental error. The deviation of the calculated magnetization from the noninteracting spin-wave prediction is illustrated in Fig. 4 for the parameters given in (6.2). The temperature dependence of  $H_A(T)$  is seen to influence  $\Delta M(T)$  by nearly the same amount as the renormalization of the energies with respect to  $J_T$  and  $J_L$ . This is a consequence of the nearly equal magnitude of  $H_A$  and  $H_L$  together with the fact that these two interactions have essentially identical effects on  $\Delta M(T)$  due to the two-dimensional character of the spin system. From the results of our calculations, as shown in Fig. 4, it is apparent that the neglect of temperature-dependent variations in  $H_A$  and  $J_L$  is valid only below 2°K. This accounts for the slightly different parameters [ $J_T/k_B$

TABLE I. Summary of three-dimensional renormalized spin-wave fit for antiferromagnetic  $\text{CrCl}_3$  in zero external field for  $J_T/k_B = 5.25^\circ\text{K}$ ,  $J_L/k_B = -0.018^\circ\text{K}$ ,  $H_A(0) = 650$  Oe, and  $\nu(0) = 63.318$  Mc/sec. The listed frequencies correspond to the  $\frac{1}{2} \leftrightarrow -\frac{1}{2}$   $^{53}\text{Cr}$  NMR.

$T$ (°K)	$\nu_{\text{obs.}}$ (Mc/sec)	$\nu_{\text{calc.}}$ (Mc/sec)	$\nu_{\text{calc.}} - \nu_{\text{obs.}}$ (kc/sec)	$\xi_T$	$\xi_L$
0.400	63.163	63.167	4	1.0000	1.0000
0.509	63.089	63.088	-1	1.0000	1.0000
0.598	63.015	63.018	3	1.0000	1.0000
0.766	62.886	62.871	-15	1.0000	1.0000
0.862	62.782	62.779	-3	0.9999	0.9926
1.007	62.628	62.634	6	0.9999	0.9905
1.141	62.501	62.492	-9	0.9999	0.9885
1.20	62.438	62.427	-11	0.9998	0.9876
1.40	62.208	62.200	-8	0.9997	0.9844
1.495	62.099	62.088	-11	0.9997	0.9828
1.60	61.942	61.960	18	0.9996	0.9809
1.805	61.697	61.703	6	0.9995	0.9772
2.00	61.450	61.449	-1	0.9994	0.9736
2.20	61.162	61.179	17	0.9992	0.9697
2.49	60.768	60.773	5	0.9989	0.9638
2.79	60.334	60.334	0	0.9986	0.9575
3.00	60.030	60.035	5	0.9984	0.9529
3.10	59.863	59.863	0	0.9982	0.9507
3.40	59.391	59.391	0	0.9978	0.9438
3.50	59.244	59.231	-13	0.9977	0.9415
3.70	58.928	58.905	-23	0.9974	0.9368
3.80	58.713	58.737	24	0.9972	0.9343
4.01	58.375	58.384	9	0.9969	0.9292
4.12	58.171	58.196	25	0.9967	0.9265
4.44	57.610	57.638	28	0.9961	0.9184
4.69	57.186	57.190	4	0.9955	0.9119
4.97	56.665	56.677	12	0.9949	0.9044
5.40	55.869	55.867	-2	0.9939	0.8927
5.70	55.279	55.284	5	0.9931	0.8842
6.07	54.518	54.546	28	0.9920	0.8735
6.64	53.365	53.370	5	0.9902	0.8565
7.54	51.401	51.406	5	0.9870	0.8282
7.75	50.897	50.930	33	0.9862	0.8214
8.13	50.051	50.053	2	0.9847	0.8088

$= 4.50^\circ\text{K}$ ,  $(E_L + E_A)/g\mu_B = 2000$  Oe] which were obtained from the noninteracting two-dimensional spin-wave fit in I.

We now turn our attention to the calculated temperature dependences of the renormalization coefficients. Figure 5 shows the variation of  $\xi_T$  and  $\xi_L$  for  $\text{CrCl}_3$  as a

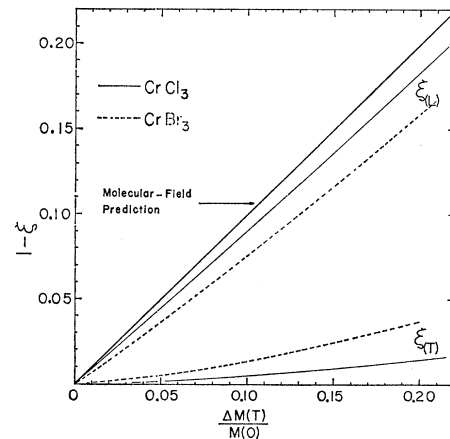


FIG. 5. The calculated variation of the renormalization coefficients for  $\text{CrCl}_3$  and  $\text{CrBr}_3$  with  $\Delta M(T)/M(0)$ .

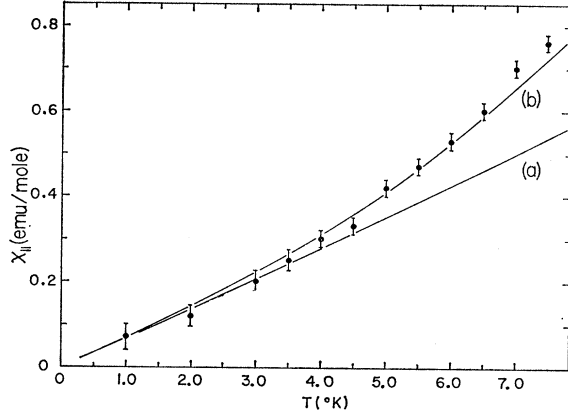


FIG. 6. Comparison of the observed and calculated parallel magnetic susceptibilities of  $\text{CrCl}_3$ . The calculated values are based on  $J_T/k_B = 5.25^\circ\text{K}$ ,  $J_L/k_B = -0.018^\circ\text{K}$ ,  $H_A(0) = 650$  Oe and (a) the noninteracting spin-wave model with temperature-independent  $H_A$ , (b) the renormalized spin-wave model with  $H_A(T) = H_A(0)[M(T)/M(0)]^2$ .

function of  $\Delta M(T)/M(0)$ . For purposes of comparison we have also shown the corresponding values for ferromagnetic  $\text{CrBr}_3$  as determined in II. The most striking feature of these plots is the strong temperature dependence of  $\xi_L$ . Particularly in the case of  $\text{CrCl}_3$  it approaches the temperature dependence of the magnetization. This result is in complete agreement with the discussion in Sec. V, concerning the validity of the molecular field approximation for the temperature dependence of  $\xi_L$  in the limit  $J_L/J_T \rightarrow 0$ . The differences between the calculated renormalization coefficients for  $\text{CrCl}_3$  and  $\text{CrBr}_3$  are thus related to the fact that  $J_L/J_T$  is considerably smaller in  $\text{CrCl}_3$  than in  $\text{CrBr}_3$ . In  $\text{CrCl}_3$  this ratio is sufficiently small that the effect of the transverse renormalization  $\xi_T$  on  $\Delta M(T)$  is quite small even at  $8^\circ\text{K}$ . It is not surprising, therefore, that a fit to our sublattice magnetization data over the whole range  $0.40 \leq T \leq 8.13^\circ\text{K}$  can be achieved with the simple two-dimensional model  $\omega'_{kt} = \omega_{(0)kt}$  (5.7) provided that both  $J_L$  and  $H_A$  are assumed to vary with temperature as  $M(T)/M(0)$ . The values of  $J_T(0)$  and  $H_A(0)$  obtained in this way do not differ significantly from those given in (6.2).

The above value of 650 Oe for the average effective  $0^\circ\text{K}$  anisotropy field clearly satisfies the requirement  $10 < H_A < 3860$ , discussed in Sec. V. That  $H_A(0)$  should lie near the lower end of this range is also reasonable since states near the lower spin-wave gap will in general have spin-wave populations disproportionately larger than those near the upper gap.

An additional check on the validity of our spin-wave model is provided by the parallel magnetic susceptibility<sup>2</sup> of  $\text{CrCl}_3$ . Because of the distribution of domain directions in the (001) plane and the small magnitude of the flop-field ( $\sim 100$  Oe), the parallel susceptibility cannot be measured by the usual methods. However, in I a method was described which makes a determination

of  $\chi_{||}$  possible. Briefly, this method consists of measuring the splitting of the  $^{53}\text{Cr}$  NMR which occurs when a weak field is applied parallel to the rf driving field and perpendicular to the  $c$  axis. The splitting for this configuration arises from a selective field-induced enhancement of the resonance. The enhancement is a maximum for those domains whose directions of sublattice magnetization make an angle  $\phi = 45^\circ$  with respect to the applied field direction. Thus the observed splitting is related to the magnitude of the field component along the sublattice directions in the following way:

$$2\pi\Delta\nu_{T,H} = 2\gamma(^{53}\text{Cr})H(\eta_{T,H} - 1) \cos(\pi/4), \quad (6.3)$$

where  $H$  is the applied field (corrected for demagnetization),  $2\eta_{T,H}$  is the absolute difference in hyperfine fields for the two opposing sublattices which is induced per unit change in magnetic field strength, and  $\gamma(^{53}\text{Cr})$  is the appropriate nuclear gyromagnetic ratio. The negative sign in (6.3) is required by the fact that the  $^{53}\text{Cr}$  hyperfine field in  $\text{CrCl}_3$  is negative.<sup>2</sup> Also, it was shown in I that  $\eta_{T,H} > 1$  at temperatures above  $1^\circ\text{K}$ . The molar parallel susceptibility was given in I as

$$\chi_{||} = \eta_{T,H} M_S / \nu(0), \quad (6.4)$$

where  $M_S = 1.67 \times 10^4$  emu/mole is the saturation magnetization at  $0^\circ\text{K}$ . We have extended our previous measurements of  $\Delta\nu_{T,H}$  to  $\sim 8^\circ\text{K}$  using applied fields  $H \leq 100$  Oe and have compared values of  $\chi_{||}$  calculated from (6.3) and (6.4) with predictions of spin-wave theory. Appropriate demagnetizing corrections ( $\frac{2}{3}\pi M$ ) for our spherical specimen were obtained by assuming a random distribution of domain directions in the hexagonal basal plane (i.e.,  $\chi = \frac{1}{2}\chi_{||}$  was assumed in calculating  $M$ ). The spin-wave predictions for  $\chi_{||}$  (5.11) were based on the parameters in (6.2). The necessary computations were performed on a CDC-1604 computer. Calculations of the zero-field susceptibility were carried out for both noninteracting and renormalized theories by substituting the appropriate dispersion laws for  $\omega_{kt}$  in (5.11). For the noninteracting theory we chose  $\omega_{kt} = \omega_{(e)kt}$  from (5.5); for the renormalized theory we chose  $\omega_{kt} = \epsilon_{(e)kt}$  from (5.28) and utilized the renormalization coefficients obtained previously (Fig. 5). Although  $\xi_T$  and  $\xi_L$  were derived for the case  $H = 0$ , the weak fields utilized in the  $\chi_{||}$  measurements are not expected to change these coefficients significantly. Our results are summarized in Fig. 6. The agreement between the renormalized theory and experiment is seen to be quite good. On the other hand the measured values of  $\chi_{||}$  above  $4^\circ\text{K}$  clearly deviate from the predictions of the noninteracting theory. The magnitude of  $\chi_{||}$  is remarkably large, in keeping with the expected labile character of a two-dimensional ferromagnetic spin-system. Finally, it should be emphasized that the calculated values of  $\chi_{||}$  did not depend on any adjustable parameters, and thus can lend support to the validity of our spin-wave model.

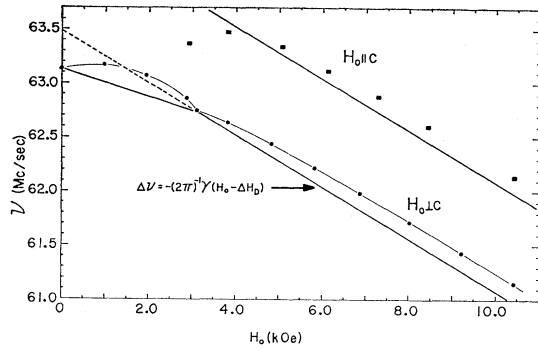


FIG. 7. Plot of the  $^{53}\text{Cr}$  NMR in a spherical specimen of  $\text{CrCl}_3$  at  $T=0.44^\circ\text{K}$  as a function of applied field strength for  $\mathbf{H}_0\parallel c$  and  $\mathbf{H}_0\perp c$ .

### B. High-Field Experiments

Because of the small interlayer exchange energy in  $\text{CrCl}_3$  it is possible, with ordinary laboratory fields, to transform the spin system from an antiferromagnet with small spin-wave gap to a ferromagnet with large spin-wave gap. It is of interest to follow the changes in the sublattice magnetization which accompany this transformation. We have made such measurements in the range  $0 < H \leq 10$  kOe at several temperatures between  $0.4$  and  $4.0^\circ\text{K}$ . Measurements were made both for  $\mathbf{H}\perp c$  and  $\mathbf{H}\parallel c$ . The changes in sublattice magnetization were deduced from frequency measurements of the  $^{53}\text{Cr}$  NMR, as in the weak-field case. Since the observations were made in fields greater than the flop-field, only frequency shifts and not splittings were detected. The procedure for extracting the sublattice magnetization behavior from the observed resonance shifts was the same as above. That is, the data were adjusted for demagnetizing effects and for shifts due to the direct interaction between field and nuclear moment. The magnitude of these adjustments can be seen clearly in Fig. 7, which shows the results of field dependence measurements at  $0.44^\circ\text{K}$ . At this temperature the sublattice magnetization is nearly saturated even in zero field. Above 7 kOe the slope  $\partial\nu/\partial H$  is found to be given exactly by  $(2\pi)^{-1}\gamma(^{53}\text{Cr})$  for both orientations of the external field. This behavior is in agreement with our spin-wave model which predicts essentially complete saturation of the sublattice magnetization for these values of  $T$  and  $H$ . The negative sign of  $\partial\nu/\partial H$  shows that the hyperfine field at the chromium nucleus is negative.

The data shown in Fig. 7 can also be used to obtain the effective demagnetizing field for our spherical specimen. The shift of the nuclear resonance due to demagnetization simply corresponds to a change in the static dipole field at the nucleus when the specimen is magnetized. At  $0.44^\circ\text{K}$  the nuclear resonance is found at  $61.149$  Mc/sec in an external field ( $\mathbf{H}_0\perp c$ ) of  $10.432$  kOe, which compares with the zero-field,  $0^\circ\text{K}$  frequency  $\nu(0)=63.318$  Mc/sec obtained from our spin-wave analysis (6.2). This frequency shift corresponds to a net

field of  $9.015$  kOe in the  $0.44^\circ\text{K}$  measurement. Thus, when the spherical sample is magnetized in the basal plane, the  $0^\circ\text{K}$  change in the dipole field at the  $^{53}\text{Cr}$  nucleus is given by

$$\Delta H_{D,1} \equiv H_{D,1}(\text{ferro}) - H_{D,1}(\text{antiferro}) = -1.417 \text{ kOe.} \quad (6.5)$$

This result is in reasonable agreement with the calculated value (4.3) of  $1.289$  kOe based on  $225^\circ\text{K}$  lattice constants. The difference is easily accounted for by thermal expansion effects. Also, using the  $225^\circ\text{K}$  x-ray density<sup>8</sup> we calculate a classical demagnetizing field for our sample  $\frac{4}{3}\pi M_S = 1.319$  kOe.

The difference in dipole fields between the perpendicular ( $\mathbf{H}_0\perp c$ ) and parallel ( $\mathbf{H}_0\parallel c$ ) magnetization directions is given by our  $0.44^\circ\text{K}$  data as

$$H_{D,1}(\text{ferro}) - H_{D,11}(\text{ferro}) = 3H_{D,1}(\text{ferro}) = 4.127 \text{ kOe.} \quad (6.6)$$

Using the calculated value (4.3) and adjusting it according to the ratio of observed to calculated values of  $\Delta H_{D,1}$ , as given above, we obtain  $3.13$  kOe. The discrepancy between the observed value (6.6) and the calculated value is clearly outside our limits of error and must be attributed to a small anisotropy in the hyperfine field. This anisotropy might be accounted for by anisotropic orbital contributions or perhaps by anisotropic magnetostrictive effects. The hyperfine anisotropy in  $\text{CrCl}_3$  is given by

$$\Delta H_{\text{hfs}}[(\parallel c) - (\perp c)] = +1.00 \text{ kOe.} \quad (6.7)$$

A similar effect in  $\text{CrBr}_3$  has been inferred by Gossard *et al.*<sup>31</sup> from the observed difference between the  $0^\circ\text{K}$  domain ( $\mathbf{M}\parallel c$ ) and domain wall ( $\mathbf{M}\perp c$ )  $^{53}\text{Cr}$  resonances. After applying corrections for differences in calculated dipolar contributions, these authors found a remainder of  $+2.03$  kOe.

The above dipolar corrections [adjusted for changes in  $M(T,H)$ ], and hyperfine anisotropy corrections, together with corrections for nuclear Zeeman shifts, were applied to our data and the resulting  $M(T,H)/M(0)$  variations are summarized in Fig. 8. These plots show two remarkable features. The first is the sharp dip in the sublattice magnetization behavior near  $1.6$  kOe. This discontinuity coincides with the field  $H_c$  at which the transformation from antiferromagnet to ferromagnet has just been completed (i.e., the canting angle of the sublattice magnetizations is  $90^\circ$ ). According to the molecular field model this occurs when  $E_H = 2E_L$ . The reasons for the dip can be found in the dispersion law for the ferromagnetic state (5.13), (5.14). The spin-wave gap, which is given by  $g\mu_B H + 2J_{LZ}LS$ , is clearly zero at this point. Since the  $\text{CrCl}_3$  sublattice magnetization is strongly influenced by the magnitude of the spin-wave gap, the minimum must be associated

<sup>31</sup> A. C. Gossard, V. Jaccarino, and J. P. Remeika, Suppl. J. Appl. Phys. **33**, 1187 (1962).

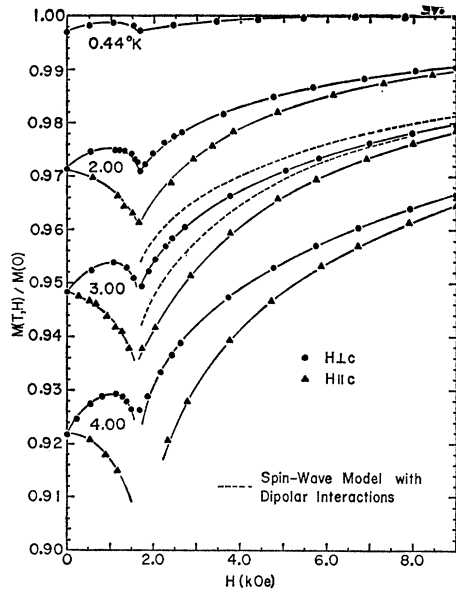


FIG. 8. The sublattice magnetization behavior of  $\text{CrCl}_3$  as a function of magnetic field strength ( $H = H_0 - 4\pi NM$ ) for  $\mathbf{H}_0 \parallel c$  and  $\mathbf{H}_0 \perp c$ .

with the disappearance of the gap at  $H = H_c$ . This gap sensitivity has already been discussed in connection with our parallel magnetic susceptibility measurements. It can also be seen in the very rapid increase in  $M(T,H)/M(0)$  with increasing field strength above  $H_c$ . It is noteworthy that the magnitude of  $H_c$  is independent of field direction; this shows that the  $\mathbf{k}=0$  anisotropy in the ferromagnetic state is quite small. We estimate from our measurements that  $H_A = 0 \pm 50$  Oe.

We have not attempted to analyze in detail the sublattice magnetization behavior in the range  $0 < H < H_c$ . It is likely, however, that the maximum ( $\mathbf{H} \perp c$ ) near the middle of this range is associated with the increase in frequency of the in-plane mode as a result of the external field.

The second remarkable feature of the sublattice magnetization plots is the large difference which is observed in the values of  $M(T,H)/M(0)$  for the two field orientations. This difference cannot be accounted for by a simple gap effect since we have already concluded that  $H_A = 0$  in the ferromagnetic state. We propose, therefore, that the measured difference is due to long-range dipolar couplings between spins. The modification of the spin-wave energies which results from these interactions was first considered by Holstein and Primakoff<sup>20</sup> for cubic lattices. The importance of these corrections has recently been emphasized by Charap and Boyd.<sup>32</sup> If we neglect dipolar interactions with near neighbors in "ferromagnetic"  $\text{CrCl}_3$  (i.e., those neighbors which contribute importantly to the static dipole field, and hence to  $H_A$ , in a spherical sample) we can follow

<sup>32</sup> S. H. Charap and E. L. Boyd, Phys. Rev. **133**, A811 (1964).

Holstein and Primakoff and take

$$e_{\mathbf{k}t} = [(\omega_{\mathbf{k}t})^2 + 4\pi g\mu_B M \omega_{\mathbf{k}t} \sin^2\theta_{\mathbf{k}t}]^{1/2},$$

$$M(T) = M(0) \left\{ 1 - (2SN)^{-1} \sum_{\mathbf{k}t} [(e_{\mathbf{k}t})^{-1} \times (\omega_{\mathbf{k}t} + 2\pi g\mu_B M \sin^2\theta_{\mathbf{k}t}) \langle n_{\mathbf{k}t} \rangle] \right\},$$

$$\langle n_{\mathbf{k}t} \rangle = [\exp(e_{\mathbf{k}t}/k_B T) - 1]^{-1},$$

where  $\theta_{\mathbf{k}t}$  is the angle between  $\mathbf{k}$  and the net magnetization  $\mathbf{M}$ . Also,  $\omega_{\mathbf{k}t}$  are the correct spin-wave energies in the absence of dipolar interactions. The increase in the spin-wave energies  $e_{\mathbf{k}t}$  relative to  $\omega_{\mathbf{k}t}$  is the result of spin-wave demagnetizing effects which vanish when the propagation direction lies along the magnetization direction. We have shown that the highest density of low-energy spin-wave states in  $\text{CrCl}_3$  occurs along the  $c^*$  axis in  $\mathbf{k}$  space (i.e., for  $k_L/k_T \gg 1$ ). It is these states which account for the strong temperature and field dependence of the sublattice magnetization. Because of the  $\sin^2\theta_{\mathbf{k}t}$  factor in (6.8) the energy of these states is raised significantly by dipolar interactions for  $\mathbf{M} \perp c$  but not for  $\mathbf{M} \parallel c$ . Consequently,  $M(T,H)$  is expected to be lower when a  $\text{CrCl}_3$  sphere is magnetized along the  $c$  axis than when it is magnetized perpendicular to the  $c$  axis, in agreement with our observations. In order to evaluate the magnitude of the expected difference we have calculated  $M(T,H)$  at  $3.0^\circ\text{K}$  by numerical methods from (6.8) as a function of  $H$ , for both field orientations. The spin-wave energies  $\omega_{\mathbf{k}t}$  were those of (5.13), (5.14). However, we used  $J_L = J_L(0)M(T,H)/M(0)$  in order to account for spin-wave interaction effects in an approximate way. The ratio  $M(T,H)/M(0)$  was taken from experiment. The calculated  $3.0^\circ\text{K}$  sublattice magnetization curves for  $J_T/k_B = 5.25^\circ\text{K}$ ,  $J_L(0) = -0.018^\circ\text{K}$ ,  $H_A = 0$  are shown in Fig. 8. The calculated field and orientation dependences are found to agree very well with our experimental results, although the calculated magnitudes are uniformly too high. This discrepancy is probably due to the neglect of near neighbor dipolar contributions to  $e_{\mathbf{k}t}$  ( $\mathbf{k} \neq 0$ ) since these interactions are expected to lower the energy of the important  $k_L/k_T \gg 1$  modes.

## VII. SUMMARY AND DISCUSSION

We have shown that the unusual magnetic properties of  $\text{CrCl}_3$  are a consequence of the two-dimensional character ( $|J_L| \ll J_T$ ) of the ordered spin system. If  $g\mu_B H_A \ll J_T z_T$  such a system has an unusually high density of low-lying states due to the anisotropic nature of the spin-wave spectrum. Indeed, in the limit  $J_L \rightarrow 0$ ,  $H_A + H \rightarrow 0$  simple spin-wave theory<sup>18</sup> predicts vanishing long-range order. The low-temperature behavior of  $\text{CrCl}_3$  can be understood by a spin-wave model which considers only isotropic exchange interactions in the presence of a weak, effective anisotropy field.

TABLE II. Comparison of spin-wave and molecular field predictions for the exchange constants (in °K) of CrCl<sub>3</sub> and CrBr<sub>3</sub>.

	Spin-wave model			Molecular field model
	$J_T z_T / k_B$	$J_L z_L / k_B$	$(J_T z_T +  J_L z_L ) / k_B$	$(J_T z_T +  J_L z_L ) / k_B$
CrCl <sub>3</sub>	15.75	-0.037 <sup>a</sup>	15.79	6.72
CrBr <sub>3</sub>	24.75 <sup>b</sup>	0.99 <sup>b</sup>	25.74	13.00

<sup>a</sup> From magnetic susceptibility measurements.  
<sup>b</sup> From II (Ref. 4).

The temperature dependence of the zero-field sublattice magnetization in CrCl<sub>3</sub> can be accurately described by a renormalized spin-wave model over the range  $T/T_N \leq 0.5$ . The exchange constants obtained in the present study may be compared with predictions of the molecular field model

$$J_T z_T + |J_L z_L| = 3T_N / 2S(S+1), \quad (7.1)$$

as shown in Table II (which also gives the corresponding values for CrBr<sub>3</sub>). The exchange constants obtained from the spin-wave fits are much larger than the molecular field values. This discrepancy is directly related to the two-dimensional character of CrCl<sub>3</sub> and CrBr<sub>3</sub>. The reduction in the ordering temperature for nearly two-dimensional ferromagnets is consistent with the results of Kramers-Opechowski calculations by Brown and Luttinger.<sup>33</sup> More recently, Lines<sup>34</sup> has investigated this problem by Green function techniques for the case  $J_L < 0$  and an anisotropy of the form  $D(S^y)^2$ . The Neél temperatures calculated by Lines for  $|J_L| < J_T$  are considerably lower than the molecular field temperatures. Furthermore, for  $|J_L|/J_T \lesssim 0.02$  the transition temperatures rapidly approach zero with decreasing  $|J_L|/J_T$  for all values of  $D$ . These results are quite compatible with the results of our spin-wave analysis of the CrCl<sub>3</sub> (and CrBr<sub>3</sub>) sublattice magnetization data.

The marginal stability of the CrCl<sub>3</sub> spin system also manifests itself in the very strong field dependence of the sublattice magnetization. The agreement between spin-wave theory and experiment for the zero-field, parallel magnetic susceptibility was shown to be excellent. The strong field dependence in the ferromagnetic state of CrCl<sub>3</sub> can also be understood by our spin-wave model, provided that account is taken of long range dipolar effects. These effects are largely absent in the antiferromagnetic state because of the much shorter effective range of the dipolar interactions in this case. Thus, the approximation which replaces all anisotropic interactions by an effective anisotropy field is expected to be much better for the antiferromagnetic state than for the ferromagnetic state.

The interlayer exchange field  $H_L$  in CrCl<sub>3</sub> is comparable in magnitude to the demagnetizing fields  $H_{D,M}$ .

<sup>33</sup> H. A. Brown and J. M. Luttinger, Phys. Rev. **100**, 685 (1955); H. A. Brown, *ibid.* **104**, 624 (1956).

<sup>34</sup> M. E. Lines, Phys. Rev. **131**, 546 (1963).

for most sample shapes. Hence measurements of the perpendicular magnetic susceptibility must be made on samples of known geometry in order to permit corrections for demagnetizing effects to be made. In the present study these corrections were applied with sufficient accuracy to yield susceptibilities from which an accurate value of the interlayer exchange constant could be obtained.

The spin-wave solutions given in this paper should be of general usefulness for many magnetic compounds, as discussed in Appendix II. The accurate application of these solutions to the CrCl<sub>3</sub> spin system requires careful attention to zone boundary and spin-wave interaction effects associated with the low energy of  $k_L \gg k_T$  states. When  $|J_L|/J_T$  becomes sufficiently small, the two-dimensional approximation to the spin-wave states of (5.1) may be useful. The errors introduced by this approximation have been evaluated in the present paper as a function of  $E_A/E_L$  and  $E_L/k_B T$ . We have shown that this approximation is sufficiently valid in CrCl<sub>3</sub> to account for its pronounced two-dimensional ferromagnetic behavior in the antiferromagnetic state.

#### ACKNOWLEDGMENTS

We wish to acknowledge helpful discussions with Dr. J. E. Schirber and Dr. D. C. Wallace. We are indebted to D. C. Barham for his valuable technical assistance in the design, construction, and operation of the experimental apparatus. We are also grateful to R. L. Rosenbaum for collecting the <sup>53</sup>Cr NMR data above 4°K.

#### APPENDIX I

We wish to find the eigenvalues of the Hamiltonian

$$\mathcal{H} = - \sum_{i i', p p'} J_{i i', p p'} \mathbf{S}_{i p} \cdot \mathbf{S}_{i' p'} - \sum_{i, p} (H + H_{A, p}) S_{i p}^z. \quad (A1)$$

We restrict ourselves to nearest-neighbor interactions in the four-sublattice magnetic structure of Fig. 1(b) and find, for  $J_L < 0$  and  $J_T > 0$ ,

$$\mathcal{H} = -J_T [\sum_{i i', \alpha \alpha'} \mathbf{S}_{i \alpha} \cdot \mathbf{S}_{i' \alpha'} + \sum_{i i', \beta \beta'} \mathbf{S}_{i \beta} \cdot \mathbf{S}_{i' \beta'}] - J_L [\sum_{i i', \alpha \beta} \mathbf{S}_{i \alpha} \cdot \mathbf{S}_{i' \beta'}] - g \mu_B [\sum_{i \alpha} (H + H_A) S_{i \alpha}^z + \sum_{i \beta} (H - H_A) S_{i \beta}^z], \quad (A2)$$

where  $H_A = |H_{A, p}|$ . The sublattices have been divided into two groups on the basis of sublattice magnetization direction. We define

$$\begin{aligned} p = \alpha = 1, 2 & \text{ for } p = 1, 2 \\ & = \beta = 1, 2 \text{ for } p = 3, 4. \end{aligned} \quad (A3)$$

We introduce boson operators in the following way<sup>35-37</sup>

$$\begin{aligned}
 S_{i\alpha}^+ &= (2S)^{1/2}[1 - (2S)^{-1}a_{i\alpha}^\dagger a_{i\alpha}]a_{i\alpha}, \\
 S_{i\alpha}^- &= (2S)^{1/2}a_{i\alpha}^\dagger, \\
 S_{i\alpha}^z &= S - a_{i\alpha}^\dagger a_{i\alpha}, \\
 S_{i\beta}^+ &= (2S)^{1/2}a_{i\beta}^\dagger[1 - (2S)^{-1}a_{i\beta}^\dagger a_{i\beta}], \\
 S_{i\beta}^- &= (2S)^{1/2}a_{i\beta}, \\
 S_{i\beta}^z &= -S + a_{i\beta}^\dagger a_{i\beta},
 \end{aligned} \tag{A4}$$

where  $a^\dagger$  and  $a$  obey the usual boson commutation relations. Carrying out the transformation we obtain

$$\mathcal{H}C = \mathcal{H}C_0 + \mathcal{H}C_1, \tag{A5}$$

where

$$\begin{aligned}
 \mathcal{H}C_0 &= E_0 - 2J_{TS}[\sum_{i\alpha, \alpha'} a_{i\alpha}^\dagger a_{i\alpha'} + \sum_{i\alpha, \beta\beta'} a_{i\alpha}^\dagger a_{i\beta'}] \\
 &\quad - 2J_{LS}[\sum_{i\alpha, \alpha\beta} (a_{i\alpha}^\dagger a_{i\beta} + a_{i\alpha} a_{i\beta}^\dagger)] \\
 &\quad + [2J_{TzTS} - 2J_{LzLS} + g\mu_B(H + H_A)] \sum_{i\alpha} a_{i\alpha}^\dagger a_{i\alpha} \\
 &\quad + [2J_{TzTS} - 2J_{LzLS} - g\mu_B(H - H_A)] \sum_{i\beta} a_{i\beta}^\dagger a_{i\beta}, \\
 E_0 &= -4NJ_{TzTS}^2 + 4NJ_{LzLS}^2 - 4Ng\mu_B S H_A,
 \end{aligned} \tag{A6}$$

and

$$\begin{aligned}
 \mathcal{H}C_1 &= J_T \{ \sum_{i\alpha, \alpha'} [a_{i\alpha}^\dagger a_{i\alpha} a_{i\alpha'} a_{i\alpha'}^\dagger - a_{i\alpha}^\dagger a_{i\alpha} a_{i\alpha'}^\dagger a_{i\alpha'}] \\
 &\quad + \sum_{i\alpha, \beta\beta'} [a_{i\beta}^\dagger a_{i\beta}^\dagger a_{i\beta} a_{i\beta'} - a_{i\beta}^\dagger a_{i\beta} a_{i\beta'}^\dagger a_{i\beta'}] \} \\
 &\quad + J_L \sum_{i\alpha, \alpha\beta} [a_{i\alpha}^\dagger a_{i\alpha} a_{i\alpha} a_{i\beta} + a_{i\alpha}^\dagger a_{i\alpha}^\dagger a_{i\beta} a_{i\beta}^\dagger \\
 &\quad + 2a_{i\alpha}^\dagger a_{i\alpha} a_{i\beta}^\dagger a_{i\beta}].
 \end{aligned} \tag{A7}$$

The sums in (A6) and (A7) whose terms connect different lattice points include only those pairs which are coupled by an appropriate exchange constant. The quadratic part (A6) of  $\mathcal{H}C$  gives rise to the usual spin-wave states of the linearized theory, while the quartic part (A7) is responsible for interactions between these states.

The eigenvalues of  $\mathcal{H}C_0$  are most easily derived by the method of Wallace.<sup>38</sup> The advantage of this method for complex lattices is the complete specification of the necessary transformations. An obvious extension of Wallace's harmonic oscillator formalism gives the following canonical transformation for the boson operators (A4):

$$\begin{aligned}
 a_{ip}^\dagger &= \frac{1}{2} \sum_{kt} T_{kpt} [b_{kt}(1 - \eta_{pt}) + b_{-kt}^\dagger(1 + \eta_{pt})], \\
 a_{ip} &= \frac{1}{2} \sum_{kt} T_{kpt} [b_{kt}(1 + \eta_{pt}) + b_{-kt}^\dagger(1 - \eta_{pt})],
 \end{aligned} \tag{A8}$$

where

$$T_{kpt} = N^{-1/2} \sum_s \exp(ik \cdot r_{ip}) \times V_{kps} \lambda_{ks}^{-1/2} W_{kst} |\omega_{kt}|^{1/2}, \tag{A9}$$

and

$$\begin{aligned}
 [b_{kt}, b_{k't'}] &= [b_{kt}^\dagger, b_{k't'}^\dagger] = 0, \\
 [b_{ki}, b_{k't'}^\dagger] &= \delta_{kk'} \delta_{it'}.
 \end{aligned} \tag{A10}$$

This transformation leads to the diagonal form

$$\mathcal{H}C_0 = E_0 + \sum_{kt} \omega_{kt} (b_{kt}^\dagger b_{kt} + \frac{1}{2}), \tag{A11}$$

where the eigenvalues of  $b_{kt}^\dagger b_{kt}$  are  $n_{kt} = 0, 1, 2, \dots$ . To obtain (A11) for our four-sublattice model we have used

$$\eta_{pt} = R_p R_t, \tag{A12}$$

where  $R_t$  and  $R_p$  are defined in (5.4) and (5.8), respectively. In order to simplify the specification of  $T_{kpt}$  we define

$$\begin{aligned}
 A &= 2J_{TzTS} - 2J_{LzLS} + E_A, \\
 B_k &= +2J_{TzTS} |\gamma_{(T)k}|, \\
 C_k &= -2J_{LzLS} \gamma_{(L)k}, \\
 E_H &= g\mu_B H.
 \end{aligned} \tag{A13}$$

Thus,

$$\mathbf{V}_k = 2^{-1/2} \begin{pmatrix} \cos\theta & (-\cos\theta)(e^{ix}) & \sin\theta & (-\sin\theta)(e^{ix}) \\ (\cos\theta)(e^{-ix}) & \cos\theta & (\sin\theta)(e^{-ix}) & \sin\theta \\ -\sin\theta & (\sin\theta)(e^{ix}) & \cos\theta & (-\cos\theta)(e^{ix}) \\ (-\sin\theta)(e^{-ix}) & -\sin\theta & (\cos\theta)(e^{-ix}) & \cos\theta \end{pmatrix}, \tag{A14}$$

where

$$\begin{aligned}
 x &= \tan^{-1}[\text{Im}(\gamma_{(T)k})/\text{Re}(\gamma_{(T)k})], \\
 \cos^2\theta &= \frac{1}{2}[1 + E_H(E_H^2 + C_k^2)^{-1/2}].
 \end{aligned} \tag{A15}$$

Also,

$$\begin{aligned}
 \lambda_{ks} &= [A + R_s(E_H^2 + C_k^2)^{1/2}] + (-1)^s B_k, \\
 R_s &= +1 \quad \text{for } s=1, 2 \\
 &= -1 \quad \text{for } s=3, 4,
 \end{aligned} \tag{A16}$$

and

$$\mathbf{W}_k = \begin{pmatrix} \cos\phi_{(+)} & 0 & -\sin\phi_{(+)} & 0 \\ 0 & \cos\phi_{(-)} & 0 & -\sin\phi_{(-)} \\ \sin\phi_{(+)} & 0 & \cos\phi_{(+)} & 0 \\ 0 & \sin\phi_{(-)} & 0 & \cos\phi_{(-)} \end{pmatrix}, \tag{A17}$$

where

$$\begin{aligned}
 \cos^2\phi_\pm &= \frac{1}{2} \left\{ 1 + \frac{E_H(A \pm B_k)}{(E_H^2 + C_k^2)^{1/2} [A \pm B_k]^2 - C_k^2} \right\}.
 \end{aligned} \tag{A18}$$

<sup>35</sup> S. V. Maleev, Zh. Eksperim. i Teor. Fiz. **33**, 1010 (1957) [English transl.: Soviet Phys.—JETP **6**, 776 (1958)].

<sup>36</sup> T. Oguchi, Progr. Theoret. Phys. (Kyoto) **25**, 721 (1961).

<sup>37</sup> R. A. Tahir-Kheli and D. ter Haar, Phys. Rev. **127**, 95 (1962).

<sup>38</sup> D. C. Wallace, Phys. Rev. **128**, 1614 (1962).

Finally,

$$\omega_{\mathbf{k}t} = \{[A - (-1)^t B_{\mathbf{k}}]^2 - C_{\mathbf{k}}^2\}^{1/2} + R_t E_H. \quad (\text{A19})$$

#### APPENDIX II

At temperatures which are sufficiently low for the kinematic interactions to be negligible, the corrections to the spin-wave energies (A19) are given by  $\mathcal{F}\mathcal{C}_1$ . Since the eigenstates of  $\mathcal{F}\mathcal{C}_0$  are an excellent approximation to those of  $\mathcal{F}\mathcal{C}$  at low temperatures we consider only those contributions of  $\mathcal{F}\mathcal{C}_1$  which are diagonal in the  $n_{\mathbf{k}t}$  representation. The transformation to this representation is accomplished by applying (A8), (A9) to (A7). A considerable simplification of the problem is achieved by assuming  $H=0$ . In this case (A9) reduces to

$$T_{\mathbf{k}pt}(H=0) = N^{-1/2} \exp(i\mathbf{k} \cdot \mathbf{r}_{ip}) U_{\mathbf{k}pt}, \quad (\text{A20})$$

where

$$\begin{aligned} U_{\mathbf{k}pt} &= U_{-\mathbf{k}pt}^* \\ &= 8^{-1/2} [-(-1)^t]^p \left\{ \frac{X_{\mathbf{k}t} + R_p R_t Y_{\mathbf{k}t}}{(X_{\mathbf{k}t} Y_{\mathbf{k}t})^{1/2}} \right\} \\ &\quad \times \exp\left\{ \frac{1}{2} i x [(-1)^t - (-1)^p] \right\}, \end{aligned} \quad (\text{A21})$$

and

$$\begin{aligned} X_{\mathbf{k}t} &= [A - (-1)^t B_{\mathbf{k}} - C_{\mathbf{k}}]^{1/2} \\ Y_{\mathbf{k}t} &= [A - (-1)^t B_{\mathbf{k}} + C_{\mathbf{k}}]^{1/2}. \end{aligned} \quad (\text{A22})$$

Using (A20)–(A22) in (A7) gives the following diagonal terms

$$\begin{aligned} \mathcal{F}\mathcal{C}_{1d} &= -(8N)^{-1} \sum_{\mathbf{k}\mathbf{k}'} \sum_{t't'} [F_{(T)\mathbf{k}t} F_{(T)\mathbf{k}'t'} \\ &\quad + F_{(L)\mathbf{k}t} F_{(L)\mathbf{k}'t'}], \\ F_{(T)\mathbf{k}t} &= 2J_T z_T \omega_{(e)\mathbf{k}t} (\omega_{(e)\mathbf{k}t})^{-1} [1 - (-1)^t |\gamma_{(T)\mathbf{k}}|] \\ &\quad \times \{b_{\mathbf{k}t}^\dagger b_{\mathbf{k}t} + \frac{1}{2} [1 - \omega_{(e)\mathbf{k}t} (\omega_{(0)\mathbf{k}t})^{-1}]\}, \quad (\text{A23}) \\ F_{(L)\mathbf{k}t} &= -2J_L z_L (\omega_{(e)\mathbf{k}t})^{-1} [2J_L z_L S(\gamma_{(L)\mathbf{k}})^2 + \omega_{(0)\mathbf{k}t}] \\ &\quad \times \{b_{\mathbf{k}t}^\dagger b_{\mathbf{k}t} + \frac{1}{2} [1 - \omega_{(e)\mathbf{k}t} \\ &\quad \times (2J_L z_L (\gamma_{(L)\mathbf{k}})^2 + \omega_{(0)\mathbf{k}t})^{-1}]\}. \end{aligned}$$

In contrast to the ferromagnetic expression which is bilinear in  $n_{\mathbf{k}t}$ , the antiferromagnetic expression for  $\mathcal{F}\mathcal{C}_{1d}$  (A23) contains, in addition, terms which are linear in  $n_{\mathbf{k}t}$  as well as terms which contribute to the ground state energy. The origin of these contributions is identical to the origin of the zero-point effects in  $\mathcal{F}\mathcal{C}_0$ . In both cases the extra terms are associated with the well-known

fact<sup>24</sup> that the elementary excitations are derived relative to a state which is not the true antiferromagnetic ground state. It can be readily verified from (A23) that this effect disappears when  $J_L=0$  since then  $\omega_{(0)\mathbf{k}t} = \omega_{(e)\mathbf{k}t}$ . Furthermore, when  $|J_L| \ll J_T$  as in the present case,

$$\begin{aligned} N^{-1} \sum_{\mathbf{k}'} (\omega_{(e)\mathbf{k}'t'})^{-1} [1 - (-1)^{t'} |\gamma_{(T)\mathbf{k}'}|] \\ \times [\omega_{(0)\mathbf{k}'t'} - \omega_{(e)\mathbf{k}'t'}] \approx 0, \\ N^{-1} \sum_{\mathbf{k}'} (\omega_{(e)\mathbf{k}'t'})^{-1} [2J_L z_L S(\gamma_{(L)\mathbf{k}'})^2 \\ + \omega_{(0)\mathbf{k}'t'} - \omega_{(e)\mathbf{k}'t'}] \approx 0, \end{aligned} \quad (\text{A24})$$

is an excellent approximation. Consequently we need only retain the bilinear terms. The corrections to the thermodynamic functions which result from (A23) can now be calculated by a renormalization process. This is accomplished by replacing number operators in (A23) by their thermal expectation values in the following way<sup>4,25</sup>

$$b_{\mathbf{k}t}^\dagger b_{\mathbf{k}t} b_{\mathbf{k}'t'}^\dagger b_{\mathbf{k}'t'} = 2n_{\mathbf{k}t} \langle n_{\mathbf{k}'t'} \rangle. \quad (\text{A25})$$

Thus,

$$\begin{aligned} \mathcal{F}\mathcal{C}_{1d} &= (4SN)^{-1} \sum_{\mathbf{k}\mathbf{k}'} \sum_{t't'} n_{\mathbf{k}t} \langle n_{\mathbf{k}'t'} \rangle \\ &\quad \times [G_{(T)\mathbf{k}t} G_{(T)\mathbf{k}'t'} + G_{(L)\mathbf{k}t} G_{(L)\mathbf{k}'t'}], \\ G_{(T)\mathbf{k}t} &= 2J_T z_T \omega_{(0)\mathbf{k}t} (\omega_{(e)\mathbf{k}t})^{-1} [1 - (-1)^t |\gamma_{(T)\mathbf{k}}|], \quad (\text{A26}) \\ G_{(L)\mathbf{k}t} &= -2J_L z_L (\omega_{(e)\mathbf{k}t})^{-1} \\ &\quad \times [2J_L z_L S(\gamma_{(L)\mathbf{k}})^2 + \omega_{(0)\mathbf{k}t}], \end{aligned}$$

which immediately gives the renormalized energies  $\epsilon_{(e)\mathbf{k}t}$  of (5.28). The variation of  $M(T)_p$  is, of course, still given by (5.8), but with  $\langle n_{\mathbf{k}t} \rangle$  given by (5.27) instead of (5.9).

It should be remarked that the spin-wave dispersion relations (A23) derived in the present work can be readily applied to any exchange coupled lattice in which ferromagnetic and antiferromagnetic exchange paths are perpendicular to each other, provided that (1) the system can be divided into two or four sublattices and (2) the interactions can be described by the Hamiltonian (A1). Examples, in addition to planar antiferromagnets, are linear antiferromagnetic or ferromagnetic chains which are coupled to neighboring chains by ferromagnetic and antiferromagnetic interactions, respectively.